CONNECTIONAL HETEROGENEITY IN THE MOUSE AUDITORY CORTICOCOLLICULAR SYSTEM

BY

GEORGIY YUDINTSEV

DISSERTATION

Submitted in partial fulfillment of the requirements
for the degree of Doctor of Philosophy in Neuroscience
in the Graduate College of the
University of Illinois at Urbana-Champaign, 2019

Urbana, Illinois

Doctoral Committee:

Professor Mark Nelson, Chair
Associate Professor Daniel Adolfo Llano, Director of Research
Professor Janice Juraska
Associate Professor Hee Jung Chung

ABSTRACT

The auditory (cochlear) nerve and a set of intricately connected brainstem nuclei, auditory thalamus and neocortical regions, all comprise the central auditory system. This system can be further described in terms of its ascending and descending components, or pathways. The ascending pathway starts with the cochlea at the periphery; it processes and then propagates the information about sound towards the auditory cortex. The descending component consists of neural pathways that originate at the top of the central auditory system's hierarchy and may exert focal and wide-spread influences at various lower levels of the ascending auditory pathway, determining or modifying how the ascending auditory information is processed. This dissertation is focused on understanding of neuroanatomical and functional organization of the corticocollicular system – one of the largest descending projections within the central auditory system.

The first chapter of this work lays out a detailed background about the auditory corticocollicular system. The focus of this chapter is on the mouse brain, however, some information is also drawn from neuroscience research on other mammalian species, when appropriate. In the second chapter, I describe the results of my first neuroanatomical study, which postulate that layer 5 and layer 6 corticocollicular neurons arise from distinct neocortical regions, with cellular distributions that only partially overlap. This organization suggests that layer 5 and layer 6 corticocollicular neurons have different functions in terms of modulating auditory processing in the midbrain. In the third chapter, a wide-field *in vivo* imaging approach is combined with neuroanatomical tracing of the corticocollicular pathway to examine the specificity of origin of layer 5 and layer 6 corticocollicular neurons in the mouse auditory cortex.

A key finding of this chapter shows that layer 6 corticocollicular neurons are likely to be more involved in carrying non-auditory or multisensory information signals to the inferior colliculus. Retrograde and viral anterograde tracing were used in the final study and are described in the fourth chapter. These experiments provided further support for differential roles of layer 5 and layer 6 corticocollicular neurons in sound processing, and plausible multisensory nature of layer 6 corticocollicular neurons. An important finding from this chapter is the dichotomy of layer 5 and layer 6 synaptic innervation of different target regions within the inferior colliculus.

Together, the results of this work add to the foundation upon which the differences between layer 5 and layer 6 corticocollicular neurons can be understood. The new organization principles of the system described in this dissertation are important for understanding the functions of the corticocollicular system, as well as how the limbic, memory and other sensory systems may affect and integrate with early-stage auditory processing.

ACKNOWLEDGEMENTS

It would take many pages to list all the people who helped me achieve all the academic and life requirements to make this work possible. First and foremost, I would like to express deep gratitude to my research advisor Prof. Daniel Adolfo Llano, for providing me with a multitude of resources and continued support, teaching me how to do good science and giving me an extra push in times when it was needed. His contagious passion for science and high standards is the main reason that I am able to stand where I stand today. Secondly, but not less importantly, I would like to say a big thank-you to the chair of my committee, Prof. Mark Nelson, whose calm guidance, support and concise, well-rounded advice were always of tremendous value to me personally and professionally. I also want to thank my remaining committee members, Prof. Janice Juraska and Prof. Hee Jung Chung. I remember coming for research advice to Prof. Juraska already during my first year of graduate school and learning about the captivating realms of the molecular biology of the brain in Prof. Chung's class early in my graduate training. Their critical input to my thesis research and my development as a scientist was extremely valuable since the very start of this Ph.D. journey.

I want to thank my secondary school biology teacher, Romanova Natalya Yuriyevna. She saw something in a child who was oddly fascinated with microscopes and living cells, and provided him with years of teaching and mentorship, often – I am sure – taking out time from her personal life and outside of paid work hours, just to prepare him for future success in science. Likewise, these words greatly apply to many of my other school teachers. I extend my thanks to an exceptional first university professor of mine, Meiramova Rabiga Gabdullayevna, who helped me overcome some of my fears and encouraged me to apply for scholarships to be able to come study abroad. She is also an excellent teacher; histology is still one of my favorite subjects, the

deeper appreciation of which started with her course. Here, I also want to thank my friend Natasha and my brother Ivan. Without their trust in me, this whole dream of studying science at the level I wanted would have never become financially feasible.

Very special words of thanks are to my co-worker and best friend Alexandria Lesicko: for her time, patience and support. It is truly amazing to have come out of graduate school not only with great knowledge, but also having made an incredible friend. Another big thank you is to my friends Gulsim, Svetik, Misha, Maja, Melissa, Glen and Ainura, who have always been there for me even though I haven't always been able to give back as much as they deserve, being busy with my studies.

Lastly, I would like to thank Prof. Diane Beck and Prof. Lori Raetzman, for their wonderful neuroscience courses and continued guidance afterwards; the Beckman Institute's Animal Care Staff, especially the supervisor Dack Shearer; the Beckman Institute Microscopy Suite and Scott Robinson for his cheerful and funny remarks during my long Neurolucida sessions; the NSP program, especially Dr. Samuel Beshers and Stephanie Pregent, and many of the current and past members of the Llano lab, for their help and patience with me.

This work is dedicated to my grandmother Taya (01/06/1936 – 11/23/2003).

TABLE OF CONTENTS

CHAPTER 1: INTRODUCTION

THE AUDITORY SYSTEM

A major goal of the field of auditory neuroscience is three-fold: to achieve a complete understanding of how the brain decodes complex sounds, to describe how auditory percepts are formed, and finally, to explain how these percepts are assigned to behaviorally relevant meanings. Although the process of decomposing sounds into their individual frequency components is already highly complex at the level of the cochlea, the central auditory system plays a major role in all three processes mentioned above (Masterton 1992). Most importantly, addressing these questions calls for a detailed understanding of the anatomical and functional organization of the auditory pathways of the brain.

The central auditory system consists of a series of brainstem, midbrain and thalamic nuclei, as well as neocortical regions. Information about sound enters the cochlear nucleus (CN) of the brainstem via cranial nerve VIII. From the CN, information reaches the superior olivary complex (SOC), which in turn projects to the nuclei of the lateral lemniscus (NLL). All three structures also project to the inferior colliculus (IC) found in the midbrain, which sends its axons to the medial geniculate body (MGB), from which all acoustic information reaches the auditory cortex (AC) (Figure 1.1) (Malmierca and Ryugo 2012).

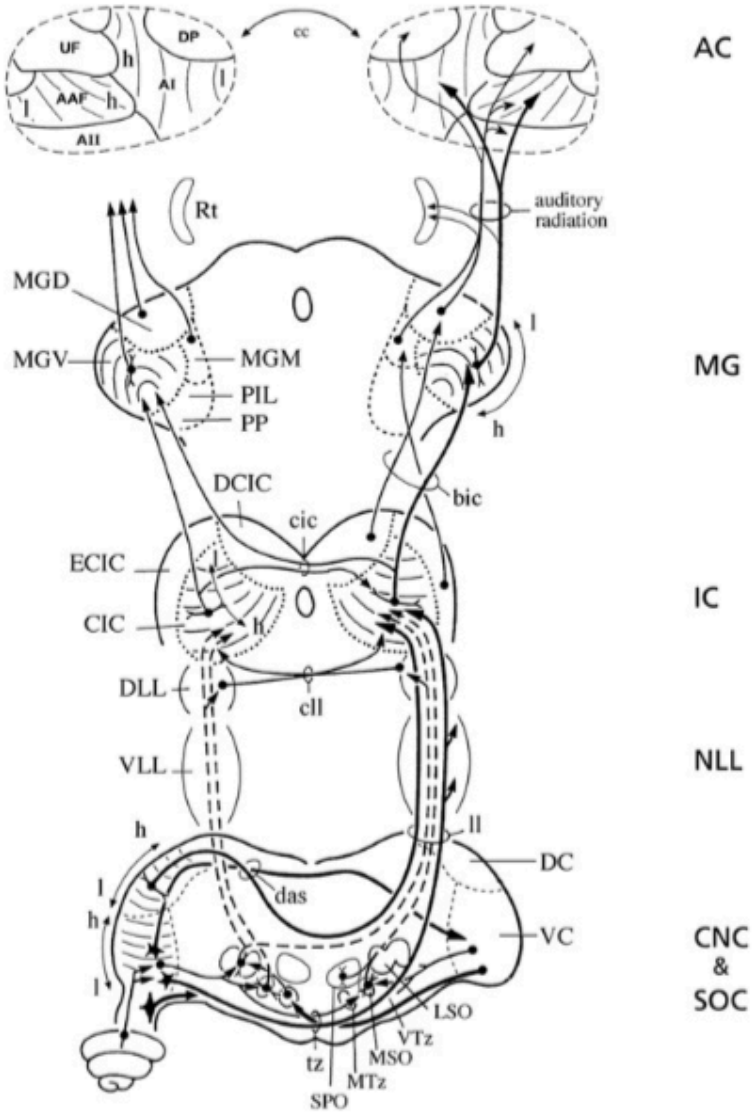

Figure 1.1. Ascending auditory pathways of the mouse *(from Malmierca and Ryugo, 2012).*

AC – auditory cortex; **MG** – medial geniculate body; **IC** – inferior colliculus; **NLL** – nuclei of the lateral lemniscus; **CNC** – cochlear nuclear complex; **SOC** – superior olivary complex. **VC** – ventral cochlear nucleus; **DC** – dorsal cochlear nucleus; **SPO** – superior paraolivary nucleus; **MTz** – medial nucleus of the trapezoid body; **MSO** – medial superior olive; **VTz** – ventral nucleus of the trapezoid body; **LSO** – lateral superior olive; **VLL** – ventral complex of the lateral lemniscus; **DLL** – dorsal complex of the lateral lemniscus; **CIC** – central nucleus of the inferior colliculus; **ECIC** – external (or lateral) cortex of the inferior colliculus; **DCIC** – dorsal cortex of the inferior colliculus; **cic** – commissure of the inferior colliculus; **bic** – brachium of the inferior colliculus; **MGV** – ventral division of the medial geniculate body; **MGD** – dorsal division of the medial geniculate body; **MGM** – medial division of the medial geniculate body; **PP** – peripeduncular nucleus; **PIL** – posterior intralaminar nucleus; **Rt** – reticular thalamic nucleus; **AAF** – anterior auditory field; **AI** – primary auditory cortex; **UF** – ultrasonic field; **AII** – secondary auditory cortex; **DP** – dorsal posterior field; **cc** – corpus callosum.

Although a clear hierarchical organization is present in the central auditory system, it is important to note that these nuclei and regions are highly interconnected with each other as well as other brain structures. The IC, for example, receives a massive set of corticofugal projections from the AC, as well as somatosensory cortical regions (Casseday, Fremouw et al. 2002, Lesicko, Hristova et al. 2016). The IC also receives subcortical feedback, particularly from the peripeduncular nucleus (PPN) and the brachium of the inferior colliculus (BIC) (Patel, Sons et al. 2017), and also itself sends descending inputs to NLL and SOC. Indeed, virtually all auditory structures relay information to higher auditory centers in the brain, while also sending feedback to the auditory structures at lower levels of this hierarchy (Figure 1.2) (Malmierca and Ryugo 2012).

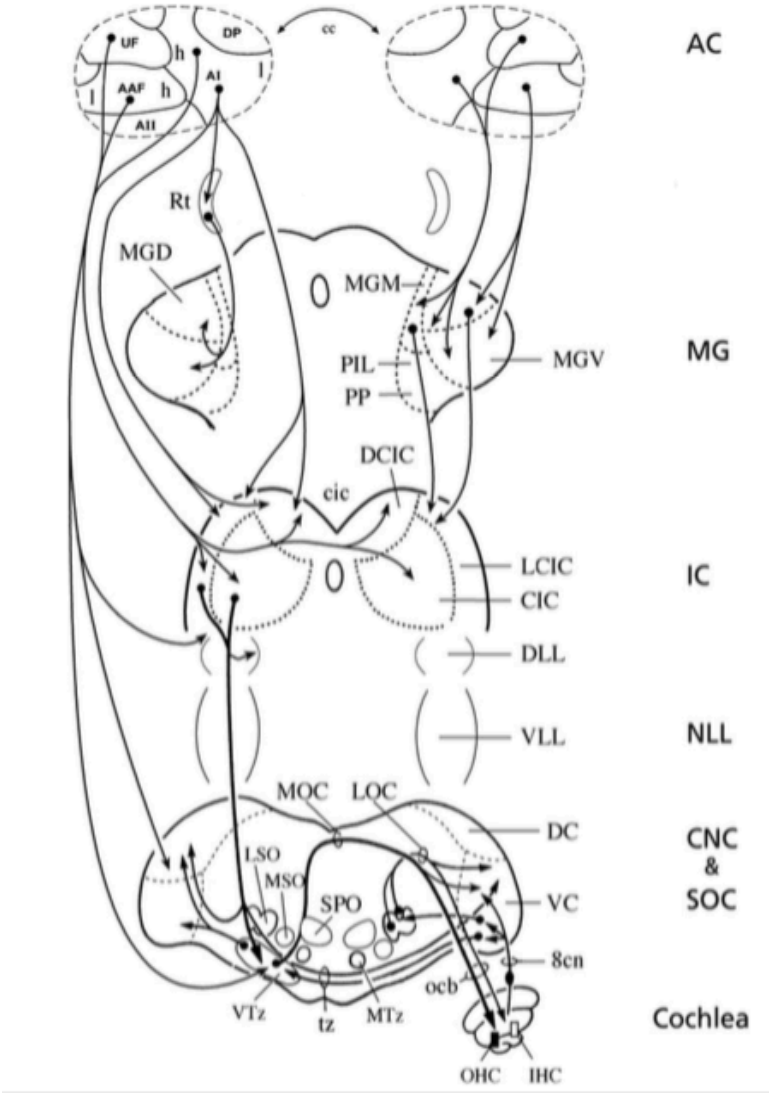

Figure 1.2. Descending auditory pathways of the mouse *(from Malmierca and Ryugo, 2012).*

AC – auditory cortex; **MG** – medial geniculate body; **IC** – inferior colliculus; **NLL** – nuclei of the lateral lemniscus; **CNC** – cochlear nuclear complex; **SOC** – superior olivary complex. **VC** – ventral cochlear nucleus; **DC** – dorsal cochlear nucleus; **SPO** – superior paraolivary nucleus; **MTz** – medial nucleus of the trapezoid body; **MSO** – medial superior olive; **VTz** – ventral nucleus of the trapezoid body; **LSO** – lateral superior olive; **VLL** – ventral complex of the lateral lemniscus; **DLL** – dorsal complex of the lateral lemniscus; **CIC** – central nucleus of the inferior colliculus; **LCIC** – external (or lateral) cortex of the inferior colliculus; **DCIC** – dorsal cortex of the inferior colliculus; **cic** – commissure of the inferior colliculus; **MGV** – ventral division of the medial geniculate body; **MGD** – dorsal division of the medial geniculate body; **MGM** – medial division of the medial geniculate body; **PP** – peripeduncular nucleus; **PIL** – posterior intralaminar nucleus; **Rt** – reticular thalamic nucleus; **AAF** – anterior auditory field; **AI** – primary auditory cortex; **UF** – ultrasonic field; **AII** – secondary auditory cortex; **DP** – dorsal posterior field; **ocb** – olivocochlear bundle; **OHC** – outer hair cells; **IHC** – inner hair cells; **8cn** – cochlear root of the vestibulocochlear nerve; **cc** – corpus callosum.

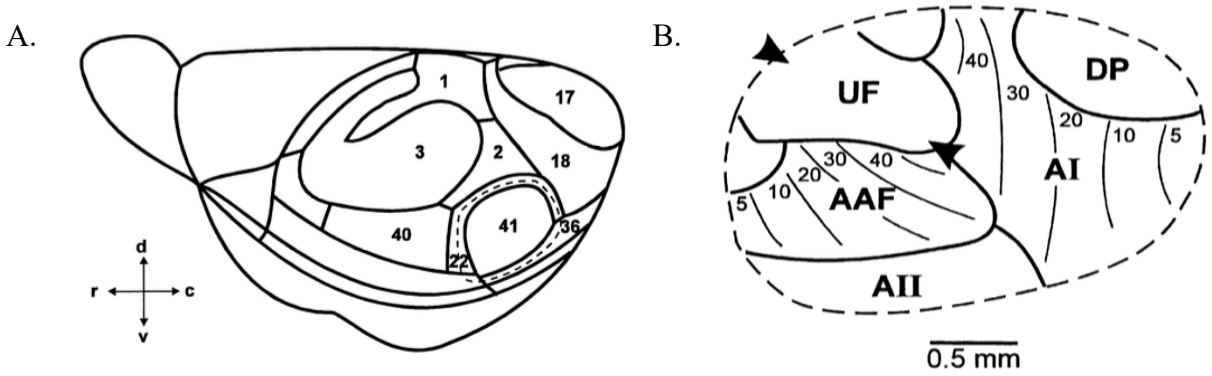

Figure 1.3. Location and regional organization of the mouse auditory cortex *(from Caviness, 1975 and Stiebler et. al., 1997).*
The mouse auditory cortex is located in area 41 (A), and can be further divided into 5 distinct fields – the anterior auditory field (AAF), the primary auditory cortex (AI), the secondary auditory field (AII), the ultrasonic field (UF), and the dorsal posterior field (DP) (B).

THE MOUSE AUDITORY CORTEX

Despite the complexity of multiple ascending and descending connections found at all levels of the central auditory pathway, the idea of hierarchical organization is a useful way to conceptualize different auditory structures of the brain. At the top of this hierarchy lies the AC. The mouse AC is localized in the temporal cortex, area 41 (figure 1.3) (Caviness 1975). It receives all of its ascending sensory input from the MGB. Therefore, one way to describe anatomically different regions of the AC is through examination of their input from the thalamus (Lee, Schreiner et al. 2004, Llano and Sherman 2008, Lee and Winer 2011). Anatomical and physiological studies of the murine AC describe at least five functionally, cytoarchitectonically and connectionally distinct areas, which can be grouped into the *core* and *belt* regions of the AC.

The Core Auditory Areas

The primary auditory cortex (A1) and the anterior auditory field (AAF), which constitute the *core* AC, are both tonotopically organized. The majority of the neurons found in the most rostral portion of the AAF and the most caudal portion of A1 are sharply tuned to low frequencies, while the majority of the neurons located in the most caudal portion of the AAF and the most rostral portion of A1 have well-tuned responses primarily to tones of high frequencies. Therefore, two tonotopic (or cochleotopic) gradients are found in the AC of the mouse, with their frequency reversal in high frequency regions (Stiebler, Neulist et al. 1997). In fact, the AC of other mammalian species possesses a similar organization, however the terminology used varies and is often species-specific. Both the AAF and A1 have been shown to receive parallel thalamic inputs from frequency-matched regions of the ventral MGB (Horie, Tsukano et al. 2013). Different and largely non-overlapping neuronal populations of the ventral MGB project to AAF and A1, respectively, and these projections are also tonotopically organized (Hackett, Barkat et al. 2011). It is also important to note that although tonotopic organization of neuronal responses to tones and topographical organization of the neuroanatomical inputs are predominant in the core AC, these are not the only organizing principles for these areas. As opposed to tonotopy, a substantial heterotopy of connections had also been found. Studies in cats quantified connections to A1 and AAF arising from distinct cortical and thalamic areas, and found that approximately 13-33% of neurons projecting to a frequency-specific location in the AC came from frequency-mismatched regions of the auditory thalamus and the ipsilateral AC (Lee, Schreiner et al. 2004).

The Belt Auditory Areas

The remaining areas of the mouse AC comprise the *belt* auditory cortex. These cortical regions include the secondary auditory field (A2), the ultrasonic field (UF), and the dorsal posterior field (DP). Two unifying features of these belt areas have been described. First, no apparent tonotopic organization has been identified in these areas, although some researchers proposed the presence of a weak tonotopy in A2 and UF (Issa, Haeffele et al. 2014). The neurons found in these regions are generally broadly tuned, have longer response latencies and higher spontaneous rates that neurons in the core (Joachimsthaler, Uhlmann et al. 2014). Second, the majority of the input to these areas comes from the dorsal and medial divisions of the MGB, as opposed to the ventral division of the MGB, which mainly innervates the core auditory regions (Honma, Tsukano et al. 2013). The UF of the mouse has also been shown to receive input from the ventral MGB, and is sometimes also described as the continuation of A1 specialized for processing high-frequency sounds (Hofstetter and Ehret 1992, Issa, Haeffele et al. 2014, Tsukano, Horie et al. 2015). The more complex responses found in the belt regions of the AC suggest a different level of sound processing in these regions. It is hypothesized that these areas respond better to more ethologically relevant sounds, such as species-specific vocalizations and some acoustic features present in mouse species-specific vocalizations, including slow frequency-modulated sweeps (Honma, Tsukano et al. 2013).

Differential Immunoreactivity in Mouse Auditory Cortex

In addition to divergence in functional and neuroanatomical connectivity, the belt and core regions of the AC can also be delineated on the basis of differential immunohistochemical reactivity. The core areas of the AC can be distinguished by their immunoreactivity for calcium

binding proteins such as parvalbumin and, to some extent, calbindin. Parvalbumin immunoreactivity is strongest in A1 and AAF (Cruikshank, Killackey et al. 2001). This study also reported a heavier staining for calbindin in the infragranular layers of the non-primary auditory fields. Different subfields of the mouse AC could also be delineated based on their immunoreactivity patterns against neurofilament protein SMI-32. A1 and AAF display particularly identifiable staining for this marker (Horie, Tsukano et al. 2015). Therefore, both the expression of parvalbumin and SMI 32 is strong in the core auditory cortical regions of the mouse brain, while the intensity of the staining for these two markers in A2, UF and DP is significantly reduced.

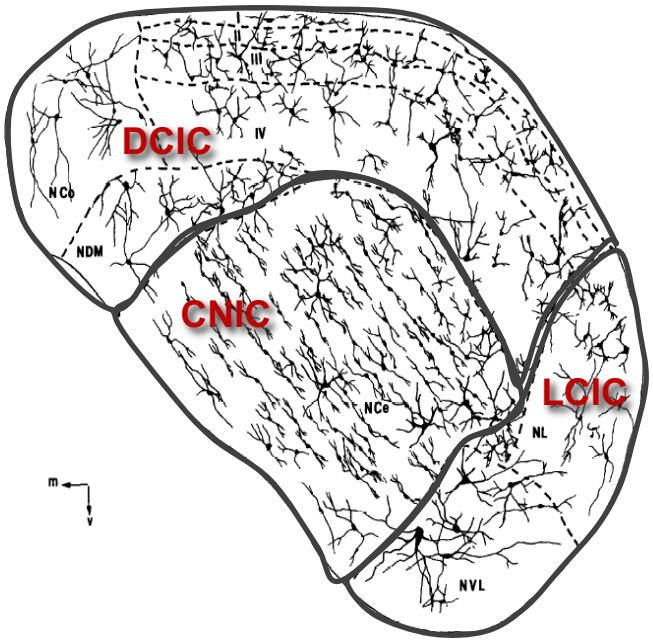

Figure 1.4. Cytoarchitecture of mouse inferior colliculus ***(modified from Meininger, Pol et al., 1986).***
The mouse inferior colliculus can be subdivided in a number of regions. The three main regions include the central nucleus (CNIC), lateral cortex (LCIC) and dorsal cortex (DCIC).
(70X)

THE MOUSE INFERIOR COLLICULUS

The IC is a part of the tectum. It is a major integration hub in a series of hierarchically arranged nuclei of the auditory pathway, and it receives information from multiple auditory and

non-auditory brain structures (Ehret 1997). The main ascending auditory input to the IC arrives from the contralateral CN. Most auditory information that enters the AC passes through the IC, with at least one exception of a non-canonical auditory pathway via the medial septum, and another example of the CN projecting directly to the thalamus (Malmierca, Merchán et al. 2002, Zhang, Sun et al. 2017). The IC also receives descending inputs from the AC, somatosensory cortex, BIC and diencephalic structures including the MGB and peripeduncular region (PP) (Lesicko, Hristova et al. 2016, Patel, Sons et al. 2017). Based on the neuropil appearance, dendritic architecture and cell size, the mouse IC can be further subdivided into at least three main subnuclei: the central nucleus (CNIC), the lateral or external cortex (LCIC) and the dorsal cortex (DCIC) (Meininger, Pol et al. 1986).

The Central Nucleus

A fundamental cytoarchitectonic feature of the CNIC is the conspicuous presence of bipolar neurons with flattened dendritic arbors and neurons of stellate morphology (figure 1.4). The bipolar cells appear disk-shaped and are arranged in concentric layers with incoming fibers, which together are often referred to as *fibrodendritic laminae*. The CNIC receives its primary sensory input from the CN, and the afferents are tonotopically organized such that the more dorsolateral aspect of the IC contains neurons and fibers tuned to low frequencies, while the neurons in the caudomedial part of the IC are tuned to high frequencies. The fibrodendritic laminae are arranged along this tonotopic gradient, and therefore are also often referred to as the *isofrequency laminae*. This organization forms the structural basis for the maintenance of the tonotopic gradient within the CNIC. Here, the bipolar cells of the CNIC are thought to integrate information of same frequency, while the stellate cells are hypothesized to play an important role

in cross-frequency integration. Other sources of ascending input to the CNIC include ipsilateral and contralateral NLL and SOC (Chen, Cheng et al. 2018). The CNIC contains both glutamatergic and GABAergic neurons, with both types projecting to the ventral MGB.

The Lateral Cortex

The LCIC surrounds the CNIC from rostral and lateral sides, although some sources specify the rostral cortex (RCIC) as a separate subdivision of the IC. Cells in the LCIC form 3 to 4 layers. Layer 1 is outer-most and contains small multipolar neurons and many passing axons. Layer 2 contains multipolar neurons of a larger size. Additionally, a unique feature of layer 2 is the presence of neurochemical and connectional modules (Wise and Jones 1977, Chernock, Larue et al. 2004). These modules are segregated patches characterized by expression of distinct neurochemical and metabolic markers such as acetylcholinesterase (AChE), glutamic acid decarboxylase-67 (GAD-67), cytochrome oxidase (CO), and nicotinamide adenine dinucleotide phosphate diaphorase (NADPH-d). Layer 3 and 4 are located more medially and contain large multipolar cells. Major ascending inputs to the LCIC include auditory and somatosensory modalities, including the NLL, CN and SOC, dorsal column nuclei and spinal trigeminal nucleus (Lesicko, Hristova et al. 2016). The LCIC of the mouse also receives descending projections from the auditory and somatosensory cortices, as well as thalamic structures such as the PP (Chen, Cheng et al. 2018). The neurons of the LCIC are broadly tuned and have longer response latencies. In the cat, many neurons have been shown to respond to both acoustic and somatosensory stimuli (Aitkin, Dickhaus et al. 1978). The LCIC also contains glutamatergic and GABAergic neurons.

The Dorsal Cortex

The DCIC is adjacent to the dorsomedial and caudal portions of the CNIC. Cytoarchitectonically, the DCIC can be subdivided into 4 layers. The outermost layer predominantly consists of passing fibers. Layers 2-4 contain multipolar neurons of various cell sizes. The most abundant input to the DCIC comes from the core and belt areas of the AC. These projections are topographical and terminate in all layers of the DCIC. This subnucleus of the IC receives a smaller descending input from portions of the thalamus, including the PP region. Ascending information about sound may reach the DCIC through the CN, NLL and SOC, as well as the CNIC (Chen, Cheng et al. 2018). Just like in the CNIC the LCIC, both glutamatergic and GABAergic neurons are found in the DCIC.

THE CORTICOCOLLICULAR SYSTEM

The presence of a direct connection between the AC and the IC had been demonstrated in many mammalian species. The neurons that mediate these connections constitute the corticocollicular system, and the more recent interest in this system arose from multiple physiological studies, which reported various changes in sound processing at the level of the IC upon AC stimulation or inactivation. Although many of these experiments were conducted in species other than the mouse, it is worth listing them here because the general principles obtained are believed to apply to other mammals as well.

First, experiments in the mustached bat and the big brown bat show that AC stimulation could modulate the tuning of neurons in the IC. As described earlier, the neurons in the CNIC as well as A1 and AAF are tonotopically organized. The corticocollicular projections are also arranged topographically according to the tonotopic gradient of the animal (Andersen, Snyder et

al. 1980), although it is not entirely clear how the topography of the corticocollicular projections relates to the isofrequency laminae found in the CNIC. When the primary regions of the AC of a given best frequency were electrically stimulated *in vivo* while responses to sound were being recorded in the CNIC, the results were downward shifts of best frequencies in the CNIC, towards the frequencies of electrically stimulated regions in the AC. Interestingly, such shifts were asymmetric, such that only the IC neurons of best frequencies higher than that of the stimulated site in the cortex, responded by shifting their best frequencies downward, in the direction of the site stimulated in the cortex (Yan and Suga 1998). These changes also lasted for a few hours after the electrical stimulation was discontinued. Similar, but slightly different phenomena were also described in the mouse. Cortical stimulation produced *corticocentric* shifts in frequency tuning of the IC neurons. In other words, the neural frequency representation in the IC was strongly enhanced for frequencies around the cortical stimulation site – more IC neurons were tuned to the best frequency of the stimulated site in A1 (Yan and Ehret 2001).

Second, the corticocollicular pathway was shown to mediate learning-induced auditory plasticity. A group of researchers led by A. King conducted a study in ferrets, which demonstrated that chromophore-targeted laser photolysis of the auditory corticocollicular projection impaired the learning function for experience-dependent recalibration of sound localization (Bajo, Nodal et al. 2010). Many animals, including the ferret, rely on binaural cues when identifying the location of a sound source. It is known that when binaural cues change, such as in case of inserting a plug in one ear, the animal's sound localization accuracy is reduced at first, but can be recovered via training. Although both the control and the experimental ferret groups in the study were able to localize sound sources accurately at first, upon the occlusion of one ear, only the animals in the control group regained their ability to localize sounds through

training sessions while one of their ears remained occluded. The group of ferrets which underwent selective ablation of the auditory corticocollicular neurons in layer 5 could not relearn to localize sounds accurately while earplug was kept in place. This learning deficit was especially prominent for sounds coming from the side ipsilateral to the occluded ear and contralateral to the lesion.

While these previous studies demonstrated the importance of the corticocollicular system for subcortical auditory plasticity, more recent experiments ascribe other functions to this projection system. In one such study, the AC was shown to control an innate sound-evoked escape behavior in the mouse through its layer 5 projections to the IC. When a subpopulation of layer 5 corticocollicular cells was activated optogenetically, flight behaviors were observed more frequently. On the other hand, when these projections were temporarily silenced during the presentation of a sound that would normally evoke a flight response in the animal, the flight responses to the alarming sound were reduced (Zingg, Chou et al. 2017). These experiments suggest that layer 5 corticocollicular cells also possess a degree of involvement in fight-or-flight response in the mouse. Yet another study shows that layer 5 corticocollicular projection may be involved in auditory gain control following the loss of peripheral auditory input (Asokan, Williamson et al. 2018). In this experiment, the mice were exposed to a high-intensity sound, which resulted in noise-induced damage to the auditory nerve synapses in the cochlea. This damage strongly correlated with increase in baseline activity of the corticocollicular neurons indicated by calcium imaging (GCaMP6s). Additionally, these layer 5 corticocollicular neurons were shown to send branches to other subcortical and corticoid structures, including the thalamus, the striatum and the lateral amygdala.

In summary, the above studies prescribe a variety of functions to the corticocollicular system, such as direct top-down control in best frequencies of IC neurons, learning-induced plasticity, escape behaviors and sensory gain control. *This functional heterogeneity is unlikely to be supported by a single type of corticocollicular neuron and calls for further understanding and characterization of the anatomy of this projection system.*

A frequently unaddressed organizational principle in many studies of the corticocollicular system is the fact that these neurons emanate from layers 5 and 6 of the temporal cortex. These descending projections primarily innervate the LCIC and the DCIC, although some studies also reported the presence of a small number of axons in the CNIC as well (Stebbings, Lesicko et al. 2014). Earlier neuroanatomical experiments describe a substantial heterogeneity of this pathway in the rat with respect to layer 5 corticocollicular neurons only. Specifically, injections of retrograde and anterograde tracer wheat germ agglutinin-horseradish peroxidase (WGA-HRP) in different regions of the CNIC (figure 1.5), LCIC (figure 1.6) and DCIC (figure 1.7) of the rat produced largely non-overlapping and in some cases complementary populations of retrogradely labeled cells in the cortex (Herbert, Aschoff et al. 1991). It was found that the CNIC receive virtually no corticocollicular input, the LCIC mainly received broad input from the secondary areas of the AC, and, finally, different layers of the DCIC were innervated by complementary but largely non-overlapping inputs from all areas of the AC.

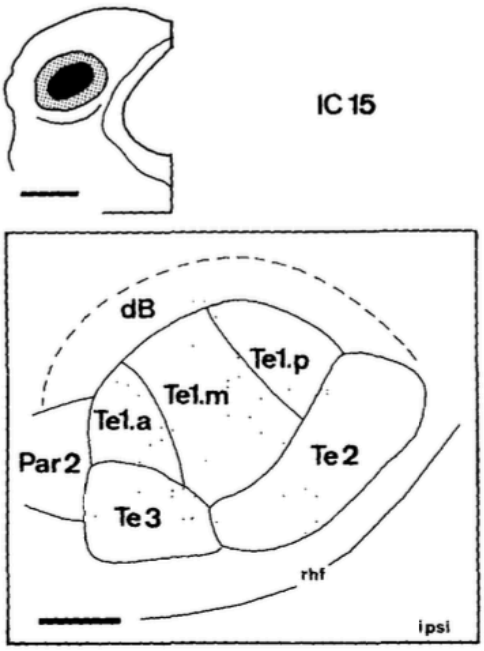

Figure 1.5. Distribution of corticocollicular neurons in the rat AC following injection of retrograde tracer in the CNIC *(modified from Herbert, Aschoff et al., 1991).*

(scale bar = 1 mm)

The rat auditory cortex consists of three primary auditory fields Te1.a, Te1.m and Te1.p, as well as surrounding secondary auditory fields Par2, Te2, Te3 and dB. Injections of WGA-HRP in the CNIC of the rat produced scarce labeling of corticocollicular cells.

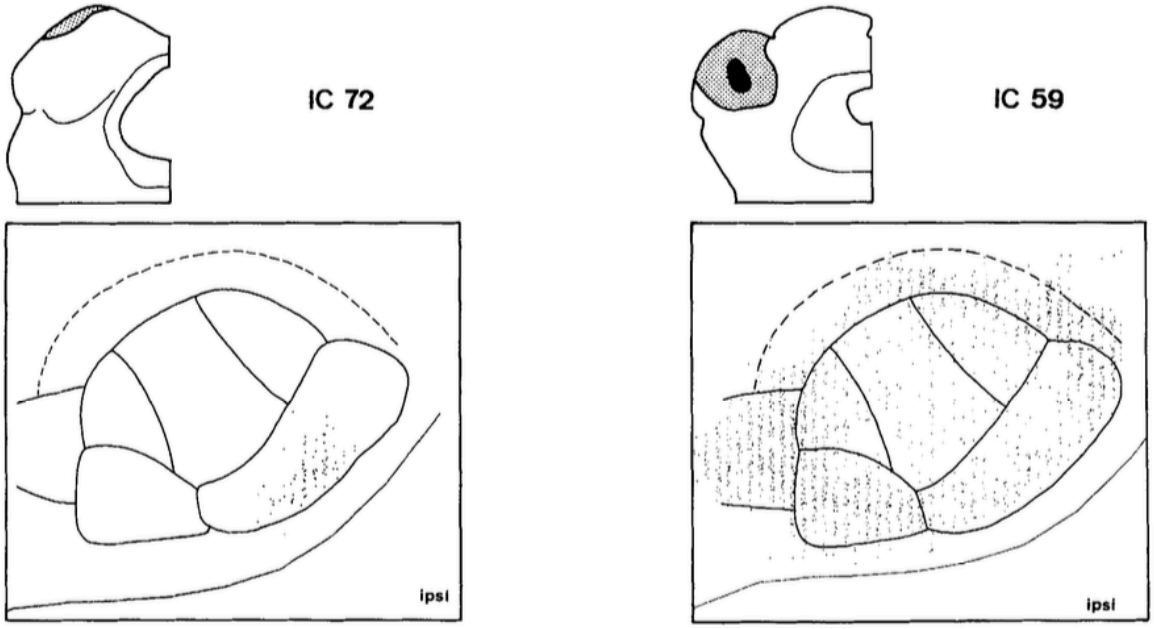

Figure 1.6. Distribution of corticocollicular neurons in the rat AC following injection of retrograde tracer in the LCIC *(modified from Herbert, Aschoff et al., 1991).*

Two examples of differential innervation by the corticocollicular neurons of the LCIC of the rat are presented. Layer 1 of the LCIC received a defined input from secondary area Te2, while more rostral portions of the LCIC are broadly innervated by many secondary areas including Te2, Te3, Par2, and dB.

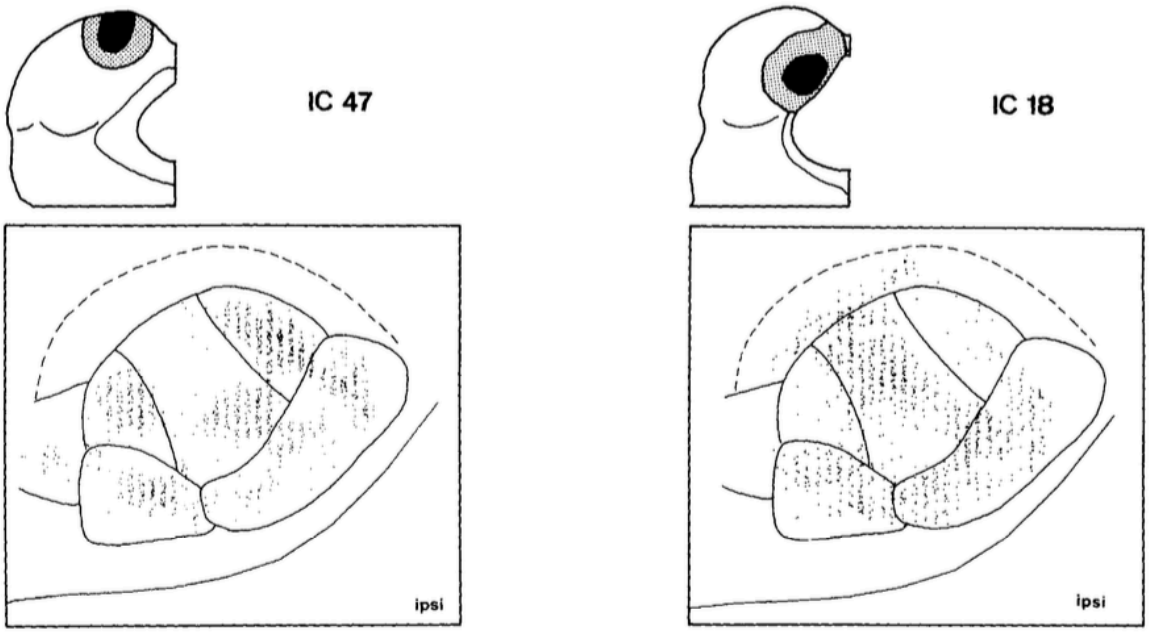

Figure 1.7. Distribution of corticocollicular neurons in the rat AC following injection of retrograde tracer in the DCIC *(modified from Herbert, Aschoff et al., 1991).*
Two examples of differential innervation by the corticocollicular neurons of the DCIC of the rat are presented. Superficial layers the DCIC received grouped inputs from all primary and secondary areas of the AC, while deeper layers of the DCIC are innervated by complimentary regions of virtually all areas of the AC.

Such heterogeneous anatomical organization of the corticocollicular projections would suggest that there is functional segregation as well. As it was described earlier, the core auditory areas of the AC are functionally and connectionally distinct from the belt auditory areas. Hence, one might predict different effects on the IC neurons mediated by these cortical areas.

Another layer of complexity of the corticocollicular system is added by projection neurons arising from the deep layer 6 of the AC, described more recently (Schofield 2009). These projections have only been recently discovered in the mouse (Slater, Willis et al. 2013). Their functional significance and anatomical organization remain largely unknown. However, the effects of this projection were likely present in some of the earlier studies of the cortical influence on the midbrain function.

In the following chapters, a set of detailed neuroanatomical and neuroimaging experiments are presented, which aim to describe and quantify the heterogeneity of the mouse corticocollicular projection. First, anatomical differences between layer 5 and layer 6 corticocollicular neurons are presented and quantified with respect to their origin in the AC. Second, a combination of *in vivo* neuroimaging and neuroanatomical serial reconstructions mark the presence of functional heterogeneity between these layers in some areas of the AC. Additionally, a new area of the temporal cortex that lies outside the AC is described, and this cortical region is shown to be connected to the IC only through layer 6 cells. Lastly, partial segregation of layer 5 and layer 6 corticocollicular efferents is achieved using a combination of viral vectors and cre-technology. This approach led to a novel insight into the morphology and innervation patterns of the corticocollicular terminals at the level of the IC.

CHAPTER 2: LAYER 5 AND LAYER 6 CORTICOCOLLICULAR NEURONS COMPRISE TWO DISTINCT AND PARTIALLY NON-OVERLAPPING DISTRIBUTIONS

INTRODUCTION

The brain is presented with a tremendous amount of sensory information, however its capacity to process this information is limited (Wood and Cowan 1995, Scalf and Beck 2010, McMains and Kastner 2011). This finite information processing capacity presents a problem of selection for appropriate stimuli while ignoring other, perhaps less relevant incoming sensory information. To overcome some of these challenges, the central nervous system of mammals evolved an elaborate set of descending projections distinct from the ascending pathways. The ascending pathways bring in sensory information from the outside world, while the descending projections arise mainly at the level of the cortex and are largely implicated in modulation of lower brain regions (O'Connor, Fukui et al. 2002, Halassa, Siegle et al. 2011, Bajo and King 2012, Terreros and Delano 2015).

Commonly referred to as top-down modulation, descending control is particularly important for the auditory system where extracting the meaning from sound is often difficult due to corruption by noise. Many studies describe the role of top-down modulation in the auditory modality. For example, high-level information about ambiguous speech has large effects on its processing (Remez, Rubin et al. 1981, Davis, Johnsrude et al. 2005, Davis and Johnsrude 2007). Moreover, the context for sound processing generated in a top-down fashion may be a general mechanism by which the auditory system disambiguates complex sounds (Lotto and Kluender 1998, Skoe and Kraus 2010). Current neuroanatomical evidence also suggests the importance of descending control for sound processing. Indeed, auditory descending projections outnumber the

ascending ones by a factor of four, emanate virtually at every level of the auditory system and project to multiple targets below their origin (Winer, Chernock et al. 2002, Winer 2005, Perales, Winer et al. 2006).

A set of projections from the AC to the IC has received much attention due to its potential ability to affect the sound processing at the level of the midbrain. Stimulation of the AC has dramatic effects on the IC neurons, including corticocentric shifts in characteristic frequency (Yan and Suga 1998, Yan, Zhang et al. 2005, Anderson and Malmierca 2013), changes in duration tuning (Ma and Suga 2001), and spectral integration (Nakamoto, Shackleton et al. 2010). These corticocollicular projections are known to emanate from two distinct infragranular layers of the cortex, namely layer 5 and deep layer 6 (Schofield 2009). More recent work described some major morphological and physiological differences between the corticocollicular neurons found in these layers (Slater, Willis et al. 2013, Slater, Sons et al. 2019), but the fundamental principles of neuroanatomical and more global functional organization of this pathway are yet to be fully described and understood. Moreover, studies in other descending systems established that the cortical layer of origin has significant implications for the function of these pathways and their effects on target structures. For example, descending projections in the corticothalamic system also emanate from layers 5 and 6. The neurons arising in these layers belong to different sub-networks of the neocortex, have different intrinsic properties and distinct projection patterns to the thalamus, and carry out different functions (Reichova and Sherman 2004, Llano and Sherman 2008, Llano and Sherman 2009, Theyel, Llano et al. 2010, Ojima and Murakami 2011).

Earlier studies described heterogeneity in layer 5 corticocollicular system (Herbert, Aschoff et al. 1991), while very few studies paid attention to a more recently discovered

corticocollicular projection emanating in layer 6 of the temporal lobe. Given mounting evidence which points to the importance of layer-specificity in describing descending pathways, I chose to compare layer 5 and layer 6 corticocollicular projections in the mouse. This chapter presents a detailed comparison of the distributions of layer 5 and layer 6 corticocollicular neurons, which reveals previously unknown heterogeneity between these two layers. More specifically, *it was hypothesized* that the global distributions of layer 5 and 6 corticocollicular neurons were partially non-overlapping. The chapter's report of my findings shows that the center of layer 6 distribution is shifted ventrally and rostrally when compared to layer 5, and the distribution of layer 6 corticocollicular neurons in the cortex is wider than layer 5. I also describe a cortical region that is connected with the mouse IC exclusively through layer 6 projection neurons.

To determine the organization of the corticocollicular projections with special attention to the cortical layer of origin, first injections of Fluorogold were performed into the left IC of BALB/c mice. Fluorogold was used here because of its established sensitivity and specificity as a retrograde tracer. Retrogradely labeled neurons were found in layers 5 and 6 of the ipsilateral cortex, as well as on the contralateral side. The focus was on the cells found on the ipsilateral side, as these neurons comprise the main component of this pathway. The brain tissue was then sectioned on a sliding microtome, and coronal sections were immunostained for parvalbumin or SMI32 to distinguish between primary and secondary AC (Mellott, Van der Gucht et al. 2010, Tsukano, Horie et al. 2015). Further, these sections were serially reconstructed in Neurolucida where distributions of layer 5 and 6 corticocollicular neurons were plotted. These reconstructions were then used for distribution analysis. It was found that the IC receives significantly non-overlapping inputs from layers 5 and 6. A considerable portion of layer 6 input originates in the rostroventral region of the temporal cortex, largely confined to non-primary areas, while layer 5

inputs come from the dorsoventral region of the AC, confined primarily to parvalbumin-and SMI32-enriched cortical regions.

MATERIALS AND METHODS

Animal Surgery and General Procedures

Adult (60-90 days) and young adult (45-60 days) BALB/c mice of both sexes were used in this study. All surgical procedures were approved by the Institutional Animal Care and Use Committee at the University of Illinois at Urbana-Champaign. Animals were housed in animal care facilities approved by the American Association for Accreditation of Laboratory Animal Care (AAALAC).

Animals were anesthetized with ketamine hydrochloride (100 mg/kg) and xylazine (3 mg/kg) intraperitoneally and placed in a stereotaxic apparatus (David Kopf Instruments, Tujunga, CA). Aseptic conditions were maintained throughout the surgery. Fluorogold (Fluorochrome, LLC, Denver, CO) was dissolved (1%) in distilled water and pressure-injected into the left IC. For iontophoretic injections, Fluorogold was dissolved in acetate buffer at pH 3.4, and injected into the left IC using iontophoresis through a 20 μm tip diameter broken glass electrode for 10-15 minutes at 10 μA positive current, with 7 s 50% duty cycle. The intent was to have a large unilateral injection into the left IC only. Cases where there was a tracer overspill to adjacent brain areas were disregarded in this study.

Fluorescence Imaging and Reconstructions

All coronal sections of the brain that contained retrograde label were serially photographed using Olympus fluorescence microscope using 5x 0.15 NA objective and UV excitation light. These images were then used to obtain 3-D reconstructions of the left AC, which was done in Neurolucida (MBF Bioscience, Williston, VT). A different marker was used for layer 5 or layer 6 corticocollicular neurons, thus keeping these populations separate for further analysis. A grid consisting of twelve rectangular bins (bin size 118,360 μm^2) was placed throughout the cortex in each coronal section, such that all layers of the cortex were covered. The rhinal fissure was used as a reference point for grid placement, with two bins of the grid being positioned below the rhinal fissure and ten above.

Immunohistochemistry

Animals were allowed to survive for 7 days post-injection. Then, the mice were deeply anesthetized with ketamine hydrochloride (100 mg/kg) and xylazine (3 mg/kg) delivered intraperitoneally and after perfused transcardially with 4% paraformaldehyde in phosphate-buffered saline (PBS) at pH 7.4. Frozen 50 µm sections were cut using a sliding microtome. Prior to cutting, three fiducial markers were placed in brain tissue along the rostro-caudal axis using a 27-gauge needle dipped into water-insoluble black India ink. For immunohistochemistry, sections were washed 3 times for 5 minutes in PBS, microwaved for 15 seconds at full power for antigen retrieval, then for 30 minutes in PBS containing 0.3% Triton-X (PBT) followed by a 30-minute blocking step in a 3% serum containing PBT solution. Blocking serum was of same species in which the secondary antibody was generated. Sections were then incubated with corresponding primary antibody overnight in the cold room. For parvalbumin (Sigma, St. Louis,

MO), 1:1000 dilution was used, and for SMI32 (BioLegend, San Diego, CA), the working dilution was 1:1500. Secondary antibody was diluted in the serum solution used for the primary wash and sections were incubated in this solution for 2 hours at room temperature. To avoid any spectral overlap with Fluorogold during imaging of the sections, Alexa-568 conjugated secondary antibody was used (Invitrogen, Grand Island, NY) to reveal SMI32 or Parvalbumin immunoreactivity. Then, the sections were washed in PBS 3 times for 10 minutes each, mounted on gelatin-coated slides, air-dried in dark room, coverslipped using fluorescence mounting medium (Vectashield H-1000, Vector labs) and sealed with nail polish.

Data Analysis

Binned cell counts for each layer were exported as Excel spread sheets. Abercrombie adjustments were done on each layer cell count separately (Abercrombie 1946). Full width at half maximum analysis of neuronal distributions along dorsoventral and rostrocaudal axes was performed as following. Cell counts for each layer were summed either along the rows or along the columns, to obtain a summary of cellular distributions in dorsoventral and rostrocaudal directions respectively. It was found that a fourth-degree polynomial provided the best fit each distribution. The centers and full width at half maximum measures were obtained for each layer in both dimensions (dorsoventral and rostrocaudal). This was done for each animal separately. Then, the half-width and the center values were analyzed using Wilcoxon Test ($n = 10$). In addition, the individual distributions for layer 5 and 6 were brought into MATLAB (MathWorks, Natick, MA) and plotted as contour maps.

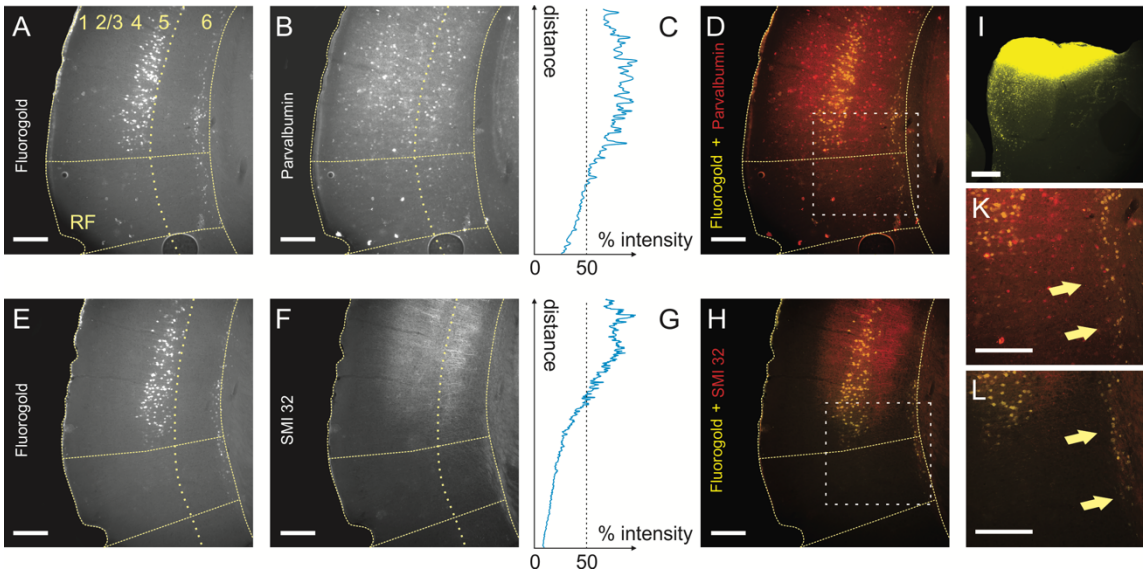

Figure 2.1. Partially segregated distributions of layer 5 and layer 6 corticocollicular neurons in mouse AC.
Corticocollicular neurons in layers 5 and 6 from adjacent coronal sections labeled with Fluorogold (A and E). Parvalbumin (B) and SMI32 (F) immunoreactivity in mouse AC. Fluorescence intensity profiles for parvalbumin (C) and SMI32 (G). Layer 5 corticocollicular neurons are strictly confined to parvalbumin-and SMI32-rich regions of the mouse AC (D and H), while a number of layer 6 corticocollicular neurons in found in parvalbumin and SMI32 negative cortical regions (D and H, also K and L). (I). Corresponding injection of Fluorogold in the left IC. Scale bar = 250 µm.

RESULTS

Fluorogold was injected into the left IC of 10 mice matched in sex and age. Seven days following the surgery, the mice were perfused, and coronals brain sections were cut on a sliding microtome. Upon examination of these sections, retrogradely labeled corticocollicular neurons were found in cortical layers 5 and 6 (figure 2.1, A and E). In six cases, the sections were also processed for parvalbumin (PV) or SMI32 fluorescent immunostaining (figure 2.1, B and F). Previous studies reported that PV and SMI32 immunoreactivity in the AC delineate primary auditory areas (Cruikshank, Killackey et al. 2001, Horie, Tsukano et al. 2015). However, no studies described the distribution of layer 5 and 6 corticocollicular neurons with respect to these neurohistological markers. Using 50% threshold for fluorescence intensity (figure 2.1, C and G),

it was observed that the majority of layer 5 corticocollicular neurons were restricted to the primary AC, while layer 6 corticocollicular neurons, particularly more rostrally, appeared in PV and SMI32 strongly and weakly staining regions, suggesting that certain cerebral cortical regions are connected with the IC only via projection neurons emanating in layer 6 (figure 2.1, D, H, and insets K and L).

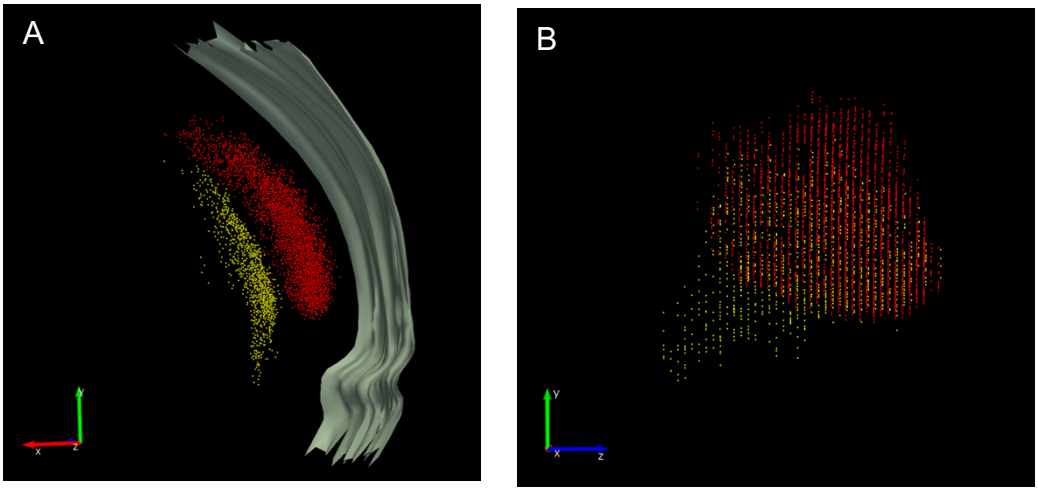

Figure 2.2. A representative reconstruction of corticocollicular cellular distributions in the cortex.
Corticocollicular neurons were marked with a red (layer 5) or a yellow (layer 6) marker. (A) A series of concatenated reconstructed coronal sections of the mouse brain on the left side. The outer grey border marks the pial surface. Rotating this reconstruction 90 degrees along the y-axis results in the lateral view of the reconstructed distributions (B). Scale bar = 250 µm.

To examine the distributions of the corticocollicular neurons further, all layer 5 and layer 6 corticocollicular neurons were plotted in Neurolucida software. Microphotographs of coronal sections containing corticocollicular neurons were serially aligned and used to create a 3-D reconstruction with plots of layer 5 and 6 corticocollicular cells (figure 2.2 A and B). Figure 2.2 shows the final result of one such reconstruction, where layer 5 corticocollicular cells are represented as red markers, and layer 6 corticocollicular cells as the yellow ones. It appeared that layer 5 and 6 corticocollicular cells were largely non-overlapping; an area containing layer 6 corticocollicular neurons without any layer 5 cells was observed rostroventrally.

Figure 2.3 (cont.)

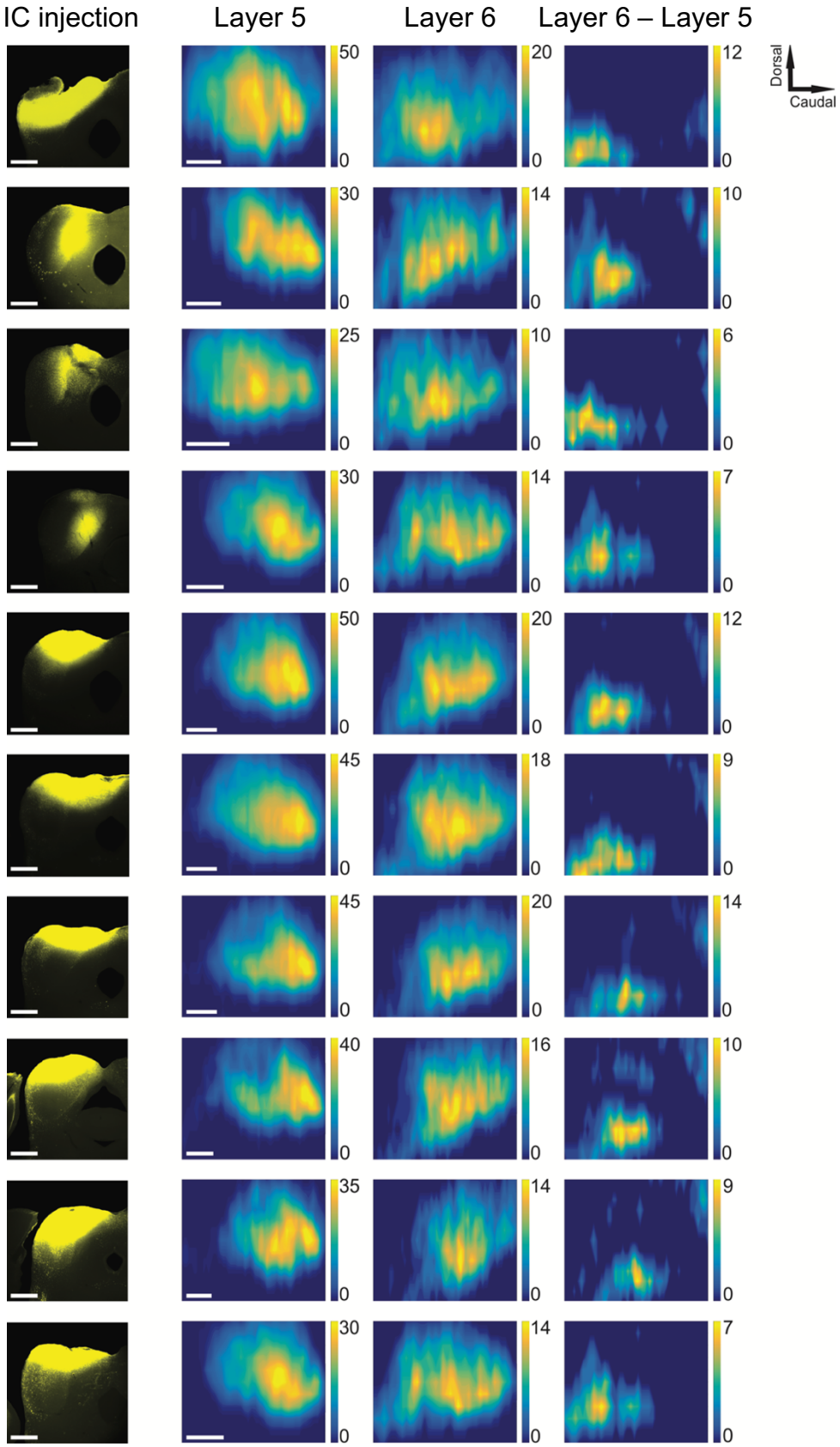

Figure 2.3. Spatial distributions of layer 5 and 6 corticocollicular neurons.
Each row includes data from one animal. The first column includes the injection sites of Fluorogold into the left IC of each animal. The second column shows the distribution of layer 5 corticocollicular neurons in the cortex, while the third column has the corresponding distributions of layer 6 corticocollicular neurons. The final column shows the difference (Layer 6 – Layer 5). The compass in the top right corner describes the directionality for the maps. Scale bar = 250 μm.

For further analyses, the distributions data were exported into MATLAB and plotted as contour maps. Figure 2.3 shows a panel with the rows corresponding to individual animals, and the columns contain the injection sites of Fluorogold in left ICs, layer 5 and layer 6 maps, and finally the difference between layers 6 and 5. Here, layer 5 cells were subtracted from layer 6, and only positive values were displayed to show regions where the number of layer 6 cells exceeded layer 5. This subtraction revealed cortical areas containing larger numbers of layer 6 corticocollicular neurons in each animal. It appears that layer 6 corticocollicular neurons occupy overall a broader area in the cortex compared to layer 5 corticocollicular neurons.

The widths and centers of the distributions for layers 5 and 6 were then compared for each animal (n = 10). The cell counts for each layer and each animal were collapsed in rostrocaudal and dorsoventral axes to obtain two distributions (figure 2.4 A and B). Along the dorsoventral axis, the average full-width at half maximum for layer 5 was 824.6 μm (SD = 57,5 μm) and 929.0 μm (SD = 92.1 μm) for layer 6 (n = 10, p-value = 0.0059, Wilcoxon signed rank test; figure 2.4 C). Along the rostrocaudal axis, the mean value of full-width at half maximum for layer 5 was 1286.8 μm (SD = 131.9 μm), and 1473.7 μm (SD = 161.9 μm) for layer 6 (n = 10, p-value = 0.0020, Wilcoxon signed rank test; figure 2.4 D). Thus, it appears that layer 6 corticocollicular neurons occupy a significantly broader area in the cortex than layer 5, suggesting that these layer 6 neurons may route distinct forms of information from cortical areas surrounding the primary AC to the IC. In addition, the center of layer 5 corticocollicular cells

was found to be displaced by 99.9 µm dorsally and 425.25 µm caudally relative to layer 6 corticocollicular cells, (n = 10, p-value = 0.0020, Wilcoxon signed rank test; figure 2.4 E), which aligns the center of the of the layer 5 corticocollicular distribution with the center of the lemniscal AC areas.

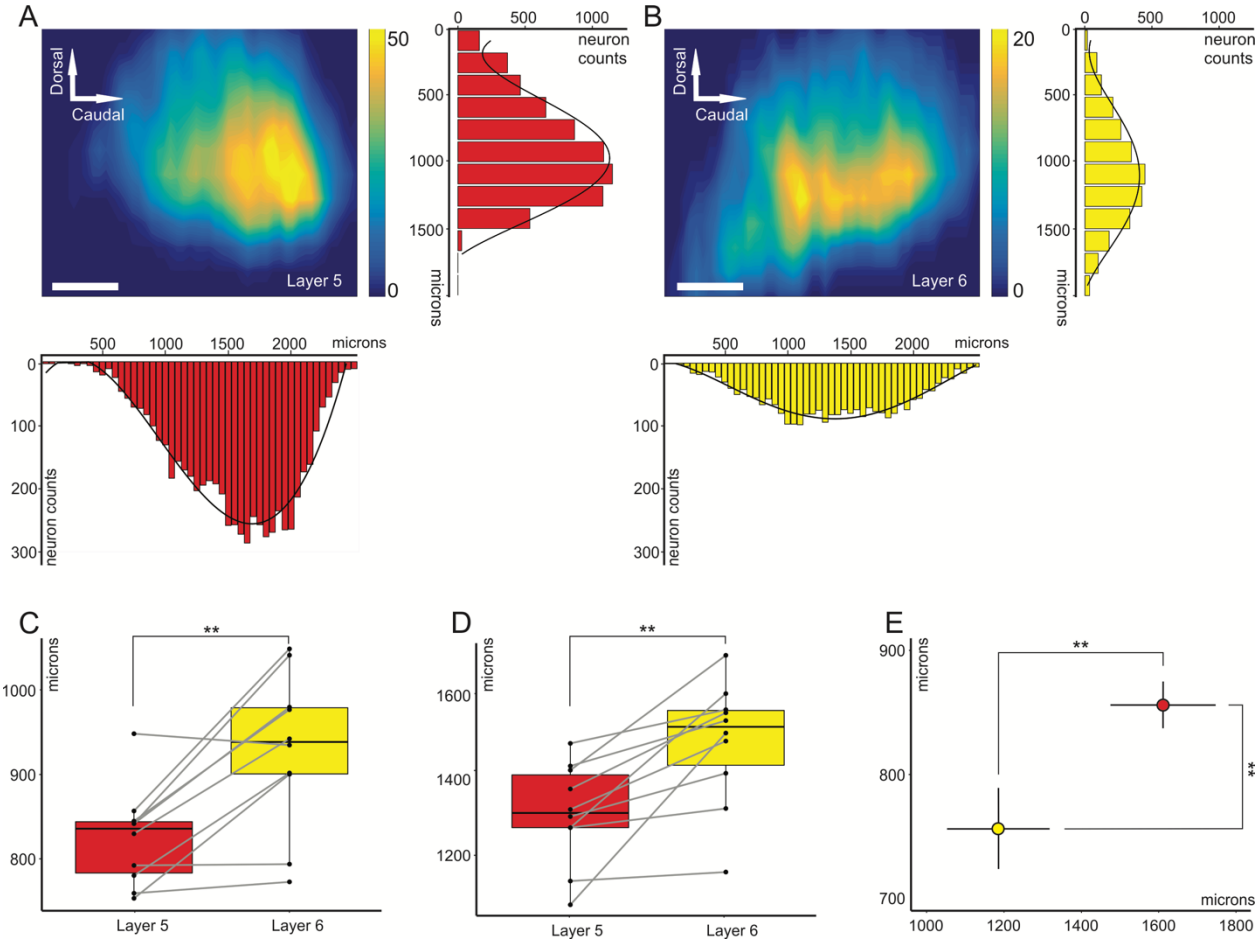

Figure 2.4. Partially segregated distributions of layer 5 and layer 6 corticocollicular neurons in mouse AC.
Distribution of layer 5 corticocollicular neurons in the neocortex, also showing the summation along the rows, which results a dorsoventral distribution, and summation along the columns – rostrocaudal distribution (A). Distribution of layer 6 corticocollicular neurons from the same animal. Although the numbers of layer 6 corticocollicular neurons are lower, they comprise a significant group (B). Comparison of full-width at half maximum measures for layers 5 and 6 in the dorsoventral direction (C) and rostrocaudal direction (D). Estimated centerss of layer 5 (red) and layer 6 (yellow) corticocollicular distributions. The center for layer 6 is shifted more ventrally and rostrally compared to layer 5. The error bars represent 95% confidence intervals (E). Scale bar = 250 µm.

DISCUSSION

The results of this chapter show that the distributions of layer 5 and layer 6 corticocollicular neurons are partially and significantly non-overlapping with respect to each other. In particular, it was found that the IC received heavy input from layer 6 from a cortical region rostral and ventral to primary IC, as indicated by staining for PV and SMI32. This region is also located near the rhinal fissure. The centers and widths of layer 5 and layer 6 corticocollicular neuronal distributions are distinct, with layer 6 encompassing a broader area of the cortex that layer 5, and its center shifted more rostrally and ventrally compared to layer 5. This organization implies that different cortical areas may modulate the IC either through layer 6 corticocollicular neurons or both layers 5 and 6.

Cell Counts and Reconstructions

This study heavily relied on a manual cell counting approach. The goal was to mark every retrogradely labeled cell in the cortex and plot those cells in 3D. Any potential cell-counting bias was addressed by using Abercrombie adjustment (Abercrombie 1946).

Distributions Analysis

The current study employed a simple form of statistical analysis for the widths and centers of the distributions for layer 5 and layer 6. Using these measures, it was possible to identify overall heterogeneity of layer 5 and layer 6 corticocollicular distributions with respect to each other. Other statistical approaches exist, however. The use of two-dimensional Gaussian distributions would provide more specific information about the nature of the distribution, including the height of the center, the position of the center value and the widths of the

distribution. However, applying this method of fitting 2-D Gaussian distributions to this data confirmed that the cellular distributions described in this study are non-Gaussian in 2-D. Therefore, I did not proceed with that method further (data not shown).

Several research groups have shown that the cortical projections from A1 to the IC are the heaviest, while the projections from non-primary areas are lighter (Herbert, Aschoff et al. 1991, Budinger, Heil et al. 2000, Bajo, Nodal et al. 2007). While mostly focusing on layer 5 corticocollicular neurons, those previous studies did not mention layer 6. In contrast, the results of this study show that non-primary auditory and non-auditory areas of the cortex send heavier layer 6 projections to the IC. Given the importance of descending projections in modulating responsiveness to sound of lower auditory centers in the brain and the importance of layer 5 and 6 projections in the corticothalamic system, it is important to consider the anatomical organization and possible functional role of both layer 5 and 6 of the corticocollicular system.

Differences between layer 5 and 6 corticocollicular distributions found in this study and previous *in vitro* recordings from these neurons point to plausible different functions of these layers in auditory cortical and midbrain processing (Slater, Willis et al. 2013). Consistent with previous findings, in this study layer 5 corticocollicular neurons also appeared to be confined to primary auditory fields as confirmed by immunostaining and imaging. Thus, these corticocollicular neurons may be the main drivers of frequency shifts and changes in tuning duration observed in the IC upon AC stimulation. Unlike layer 5, the non-overlapping area of layer 6 corticocollicular neurons found rostrally and ventrally may be important for integrating information from other sensory modalities. Likely candidates for the origin of these projections are the perirhinal area and temporal association area (Suzuki 1996). These layers 6 corticocollicular neurons would be preferentially positioned to receive multisensory information

from upper layers of these association areas and then route these signals to the IC, thus adjusting neural activity in the auditory midbrain with the information from other sensory modalities. In the following chapter, further neuroanatomical and *in vivo* imaging experiments address the nature of layer 6 corticocollicular projections with respect to cortical areas of origin.

CHAPTER 3: A SUBPOPULATION OF LAYER 6 CORTICOCOLLICULAR NEURONS ARISES FROM A NON-AUDITORY CORTICAL REGION

INTRODUCTION

The mouse AC is organized into five different regions, which include the previously mentioned primary auditory cortex (A1), anterior auditory field (AAF), secondary auditory cortex (A2), ultrasonic field (UF) and dorsal posterior regions (DP). The functional organization of these fields is thought to be maintained throughout the cortical columns. In the following set of experiments, I sought to combine the functional mapping of the mouse AC with the anatomical distributions of layer 5 and layer 6 corticocollicular neurons. The goal of these experiments was to co-localize the anatomical distributions of the corticocollicular neurons with large-scale functional maps of the mouse AC to gain new insight into the differences between layer 5 and 6 corticocollicular cells with respect to cortical areas of origin. *The main hypothesis of this chapter was that given the broader distribution of layer 6 corticocollicular neurons in the cortex, some layer 6 corticocollicular neurons will reside outside the auditory areas.* Immunohistochemical assays from Chapter 2 also support this hypothesis: a distinct group of layer 6 corticocollicular cells was found in PV and SMI32-negative regions of the mouse temporal cortex. By combining the anatomical methods from the previous chapter with *in vivo* imaging in GCaMP6s-Thy1 transgenic mice, it is shown here that a rostroventral area to the mouse AC, which contains layer 6 corticocollicular cells only, does not respond to sound stimuli, including various combinations of pure tones and species-specific mouse calls. Finally, the anatomical inputs to this cortical region were mapped using a highly sensitive retrograde tracer, Alexa-594-conjugated CTb. Consistent with the functional maps of sound-evoked activity in the cortex, this region did not get its input from any of the subdivisions of the MGB. Instead, the

amygdala and non-auditory intralaminar thalamic nuclei were the main source of inputs to this area.

MATERIALS AND METHODS

Macroscope and Imaging Set-Up

Imager 3001 Integrated data acquisition and analysis system (Optical Imaging Ltd., Israel) was used to image the cortical responses to sound in mice. C57BL6J-Tg(Thy1-GCaMP6s)GP4.3DkimJ mouse line was purchased from Jackson Laboratories. A macroscope consisting of 85 mm f/1.4 and 50 mm f/1.2 Nikon lenses was mounted to an Adimec 1000m high-end CCD camera (7.4 x 7.4 μm pixel size, 1004 X 1004 pixels, 10 frames/second), and centered above the left AC, focused approximately 0.5 mm below the surface of the exposed skull. The macroscope system had two main significant advantages over microscope objectives for large-scale imaging of the cortex: it provided a longer working distance between the specimen and the lens and 100-700 fold increase in brightness (Ratzlaff and Grinvald 1991). Blue excitation (450 nm, 30 nm band-pass), green emission (515 nm, long-pass) filters and a 495 DRLP dichroic mirror were used. Imager 3001 VDAQ software controlled the acquisition and stimulus trigger.

Acoustic Stimulation

Acoustic stimuli were generated using a TDT system 3 with an RP 2.1 Enhanced Real-Time Processor and delivered via an ES1 free field electrostatic speaker (Tucker-Davis Technologies, FL, USA), located approximately 8 cm away from the contralateral ear. All

imaging experiments were conducted in a soundproof chamber. 500 ms pure tones of 5, 10, 20, and 30 kHz were used, 100% amplitude-modulated at 20 Hz. In another set of experiments, a series of species-specific mouse calls was used as auditory stimuli. These recordings were used by previous investigators (Grimsley, Monaghan et al. 2011). Four calls from three major groups were selected. Two calls (call 1 and 2) were from a group of low-frequency stress calls. Another call (call 3) was a medium-frequency stress call, which the animals produce when restrained. The final call used (call 4), was a mating call. All playbacks were sampled at 200 kHz. Call 1, 3 and 4 were ~500 ms in duration, call 2 is ~300 ms.

Animal Preparations

All surgical procedures were approved by the Institutional Animal Care and Use Committee at the University of Illinois at Urbana-Champaign, and animals were housed in animal care facilities approved by the American Association for Accreditation of Laboratory Animal Care (AAALAC). Every attempt was made to minimize the number of animals used and to reduce suffering at all stages of the experiments.

C57BL6J-Tg(Thy1-GCaMP6s)GP4.3DkimJ mice were purchased from Jackson Laboratories, and bred as heterozygous in the local animal facility. Prior to the experiments, mice were genotyped for the presence of Tg(Thy1-GCaMP) transgene (forward PCR primer CAT CAG TGC AGC AGA GCT TC, reverse PCR primer CAG CGT ATC CAC ATA GCG TA). Before the start of the surgery, mice were anesthetized with a mixture of ketamine and xylazine (100 mg/kg and 3 mg/kg respectively) delivered intraperitoneally using a 27-gauge needle, following by an intraperitoneal injection of acepromazine (2-3 mg/kg). We found that the addition of acepromazine provides deeper and longer duration anesthesia. After the animals were

anesthetized, proper care was taken to maintain the body temperature within the range of 35.5 and 37 ºC, using a DC temperature controller (FHC, ME, USA). A skin incision over the dorsal portion of the skull was made, after which the skull was exposed. The dorsal surface of the skull was roughened using a small surgical drill bit. The area was cleaned of any remaining bone pellets, and a small aluminum bolt of 1 cm in length was secured to the surface using dental cement (3M ESPE KETAC). When the cement was set (~after 10 min), the animal was carried into a dark sound-proof chamber for imaging.

Once the imaging was complete, Fluorogold was injected into the left IC of these mice. Three additional fiducial markers were created by iontophoresis of small amounts of tetramethylrhodamine 10,000 MW dissolved in PBS (Invitrogen, Grand Island, NY) into the cortical regions outside the AC. The iontophoretic injections lasted for 4 minutes, were done through unbroken glass tip electrode with 5 μA positive current and 7 s 50% duty cycle, for 4 minutes. Using the same settings as during *in vivo* imaging, a micrograph of the skull surface was taken to aid in co-registration of functional maps with the reconstructions in Neurolucida later. The animals were allowed to survive for 7 days, after which the brain tissue was processed in same way as described in Materials and methods section of Chapter 2.

Image Analysis

Custom-written MATLAB software was used to obtain *ΔF/F* -responses to pure tones (5, 10, 20, and 30 kHz) and species-specific mouse calls. The *ΔF/F* metric was calculated according to the following equation:

$$\frac{\Delta F}{F} = \left(\frac{F_1 - F_0}{F_0}\right)_{sound} - \left(\frac{F_1 - F_0}{F_0}\right)_{silence}$$

Where:

F_1 – average fluorescence during stimulus presentation, or lack of there-of for silent trial. This metric reflects average neural activity level during the 6^{th} second, when the sound stimulus is presented.

F_0 – average fluorescence preceding stimulus presentation, or baseline activity. This metric reflects average neural activity level for from 0^{th} to 5^{th} second, before the presentation of the sound stimulus.

In this way, multiple auditory cortical regions could be identified. 2.5 standard deviations final threshold was used as a cutoff point to display the peaks of neural signals signal.

RESULTS

Given the global anatomical differences between layer 5 and 6 corticocollicular neuronal distributions described and quantified in Chapter 2, the next aim was to understand how local responses to sound map onto these anatomical distributions of layer 5 and 6 corticocollicular cells. First, the left AC of GCaMP6s-Thy1 mice was mapped by imaging responses to amplitude-modulated pure tones at 5, 10, 20 and 30 kHz using wide-field transcranial optical imager system (figure 3.1 panels A and B). Four auditory subfields were reliably identified, with A1 and AAF organized tonotopically, converging in high frequency regions near weakly tonotopic A2. UF was located dorsally, and only responses to frequencies above 20 kHz were present in this field (figure 3.1 B, C). After the imaging was complete, a retrograde tracer (Fluorogold) was injected into the left IC of these mice. Upon 7-day survival, mice were deeply anesthetized, perfused transcardially and processed for histology. Complete reconstructions of layer 5 and 6

corticocollicular distributions were done in Neurolucida (figure 3.1 D, E), and previously recorded responses were overlaid with layer 5 and 6 distributions (figure 3.1 F, G).

The combination of *in vivo* imaging and neuroanatomy proved to be useful in gaining functional insight into the organization of the corticocollicular system. Specifically, a rostroventral cortical area containing primarily layer 6 corticocollicular neurons appears outside the main auditory regions.

Next, the same techniques were applied to examine the responses of the AC to more ethologically relevant sounds (Grimsley, Sheth et al. 2016). A collection of species-specific mouse calls was used as stimuli. Again, after obtaining the reconstructions of layer 5 and 6 corticocollicular cells and overlaying this reconstruction with functional mapping, it was found

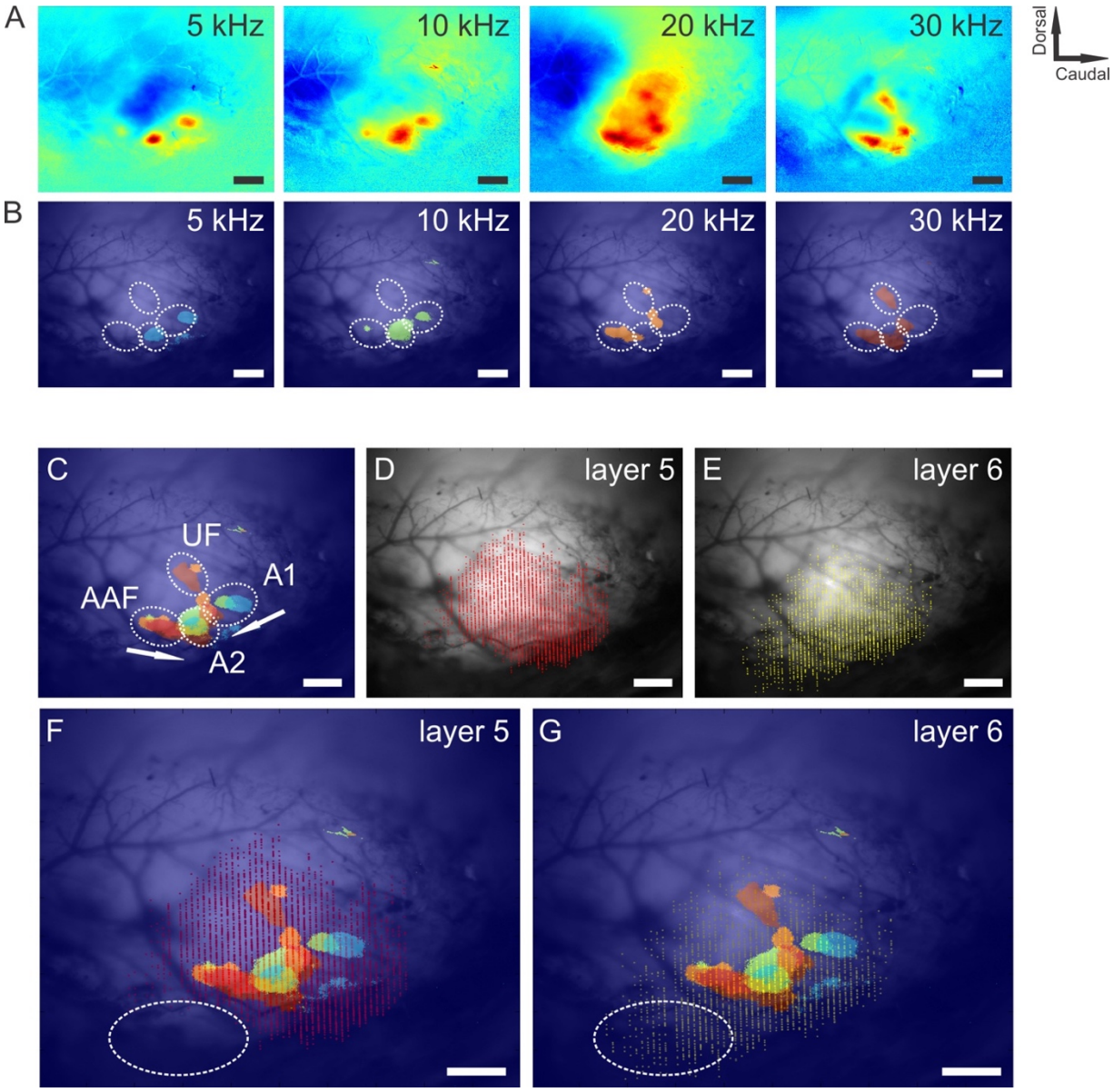

Figure 3.1. Functional maps and corresponding distributions of layer 5 and layer 6 corticocollicular neurons in mouse AC.
ΔF/F responses to 100% amplitude-modulated pure tones in mouse AC (A). A threshold level at 2.5 standard deviations was set to responses in A to display the peaks of stimulus-evoked cortical activity (B). Combination of cortical responses at threshold level from (B) identifies different auditory regions: tonotopically organized A1 and AAF, as well as A2 and UF (C). Reconstructions of layer 5 (D) and layer 6 (E) corticocollicular neurons for the same mouse. (F) and (G) are overlays of the tonotopic map and corticocollicular reconstructions. Notice the absence of sound-evoked activity in the rostroventral to AC regions (highlighted in dashed oval). Scale bar = 500 µm.

that the rostroventral to the AC area enriched in layer 6 corticocollicular cells was outside sound-responsive functional cortical areas (figure 3.2).

Finally, the inputs to this cortical region of interest were examined. Two different retrograde tracers were used for these double-tracer injection studies. Fluorogold was injected into the left IC, while Alexa-594-conjugated CTB was injected into the rostroventral region where only layer 6 corticocollicular cells were located. The distribution of the inputs from one of these experiments is presented in figure 3.3. Consistent with the in vivo neuroimaging findings, the rostroventral region received the majority of its input from non-auditory structures, including the lateral nucleus of the amygdala (LA), nucleus of the brachium of the IC (BIC), posterior limiting nucleus of the thalamus (POL), suprageniculate nucleus (SGN), and posterior complex of the thalamus (PO). These connectivity findings are indicative of non-auditory nature for this cortical area.

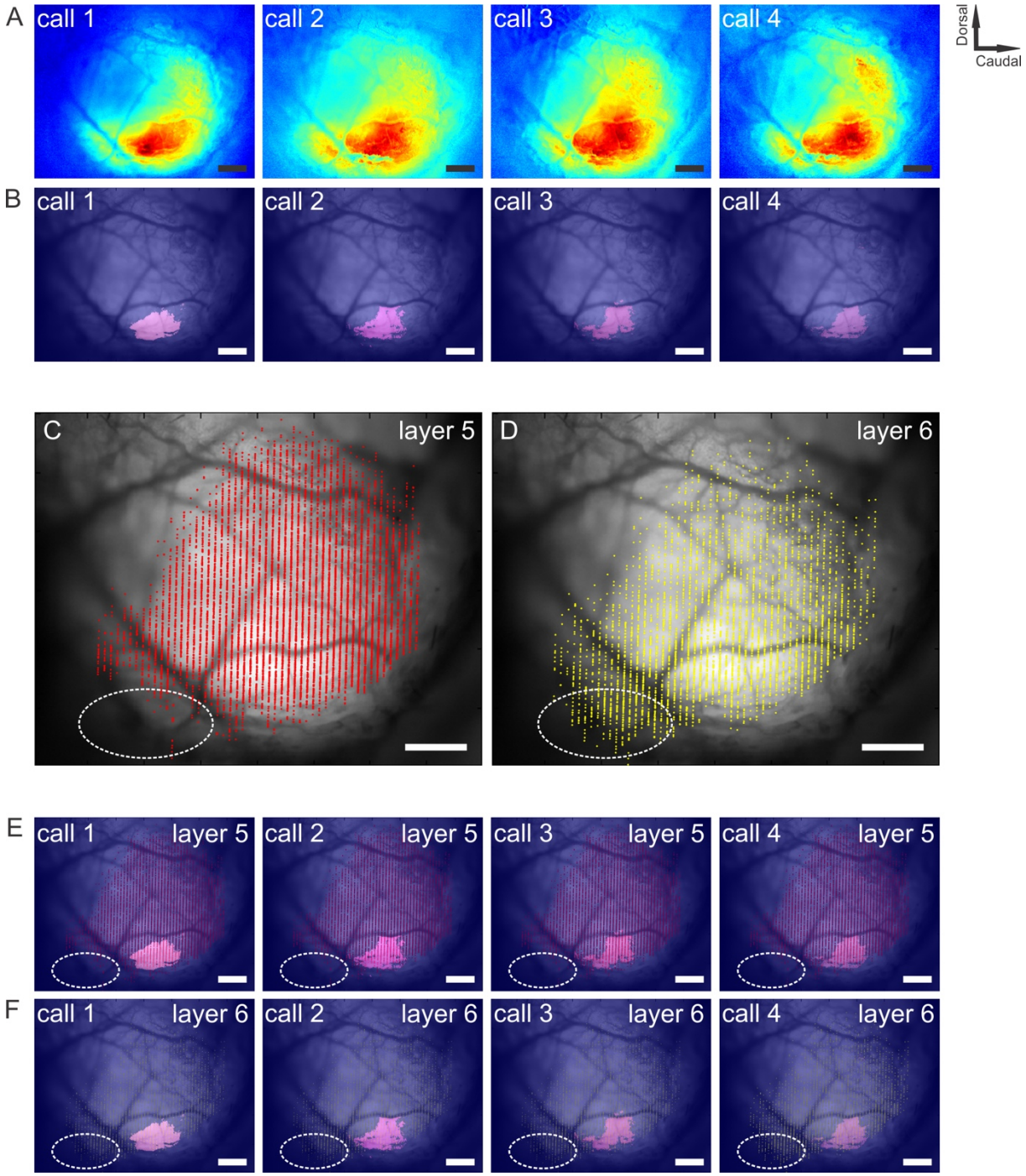

Figure 3.2. Functional responses to ethologically-relevant sounds and corresponding distributions of layer 5 and layer 6 corticocollicular neurons in mouse AC.
ΔF/F responses to four classes of species-specific calls (A). Call 1 and 2 are low-frequency stress calls, call 3 is a restraint stress-induced medium-frequency call, and call 3 is a mating call. A threshold level at 2.5 standard deviations was set to responses in A to display the peaks of stimulus-evoked cortical activity (B). Distributions of layer 5 and 6 corticocollicular cells (C, D). Overlays of functional maps from (B) with layer 5 (E) and layer 6 (F) corticocollicular cells. Scale bar = 500 μm.

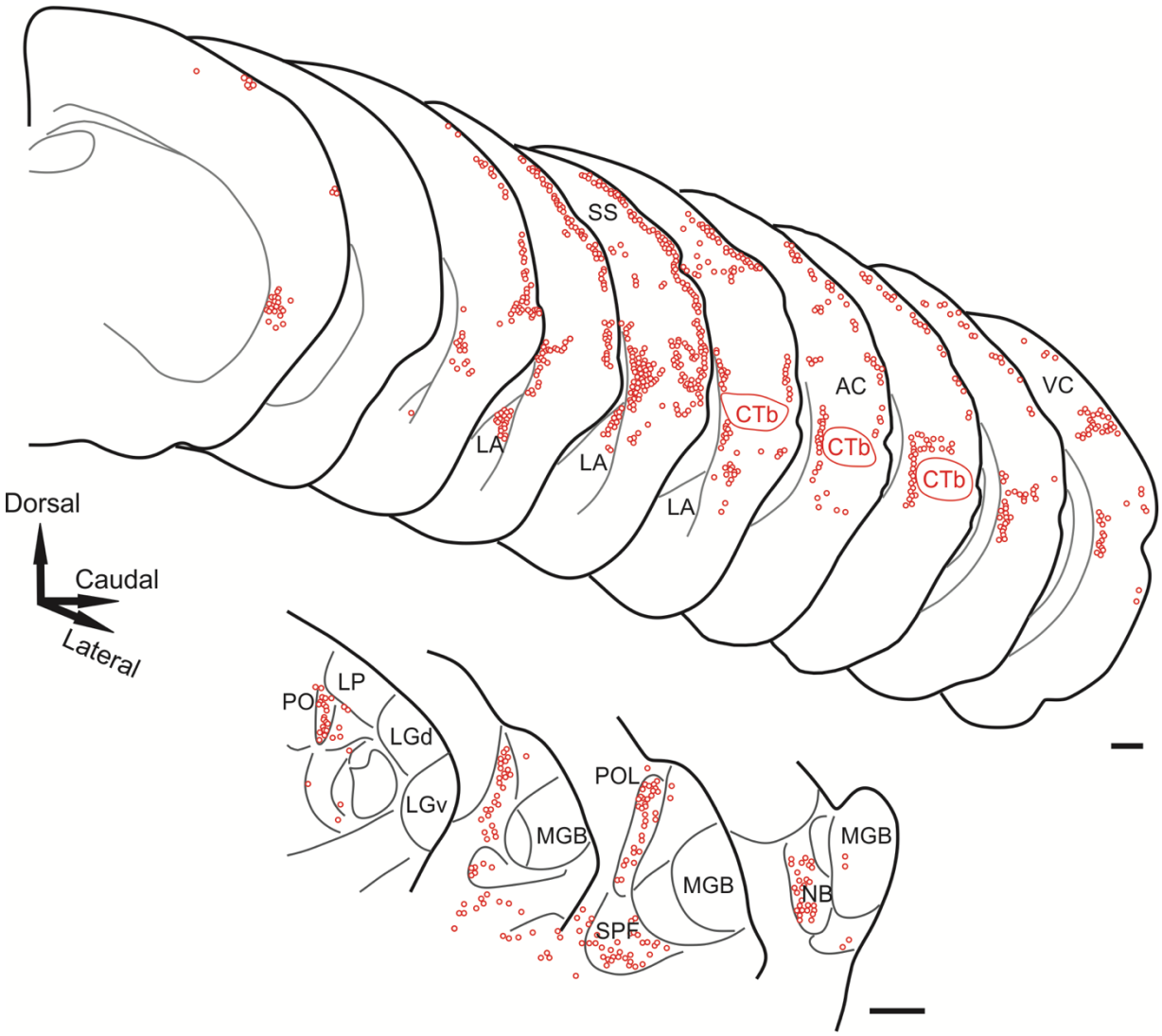

Figure 3.3. Inputs to the cortical area containing layer 6 but not layer 5 corticocollicular neurons.
The top panel shows the injection site (CTb) and cortical areas where retrogradely labeled neurons were found. A significant portion of inputs came from the lateral nucleus of the amygdala (LA), as well as somatosensory and visual cortices (SS and VC, respectively). The bottom panel shows the distribution of neurons in the thalamus and associated structures. The majority of labeled neurons were found in the posterior complex (PO), posterior limiting nucleus (POL), subparafascicular nucleus (SPF) and nucleus of the brachium of the IC (NB), but not the medial geniculate body (MGB) Scale bar = 500 µm.

DISCUSSION

Layer 5 and layer 6 corticocollicular neurons appear to be differentially distributed with respect to functionally mapped areas of the AC. More specifically, an area of the cerebral cortex

located rostrally and ventrally to the mouse AC contains layer 6 but not layer 5 corticocollicular neurons. This cortical region does not respond to sound stimuli such as pure tones of different frequencies, neither is it responsive to more ethologically relevant sounds such as species-specific calls. Four regions of the mouse AC could be distinguished based on their responses to pure tones. A1 and AAF were tonotopically organized consistent with previous reports (Stiebler, Neulist et al. 1997, Tohmi, Takahashi et al. 2009, Issa, Haeffele et al. 2014). The ultrasonic frequencies pure tones activated neurons in the UF, while all pure tone stimuli also activated A2, located ventrally to A1 and AAF gradient convergence. These regions overlapped more so with the distributions of layer 5 corticocollicular neurons, and less with the corticocollicular neurons emanating from layer 6. The four types of mouse-specific calls used in this study activated neurons located primarily in A2. Again, this activation did not overlap with the cortical area containing only layer 6 but not layer 5 corticocollicular cells.

Finally, the inputs to this area of non-overlap were described. Consistent with the functional mapping, this area of the cortex did not receive any input from the primary or higher order auditory thalamic nuclei. Instead, intralaminar nuclei were the main source of thalamic input here. The lateral nucleus of the amygdala also sent a heavy projection to this area. Although the exact behavioral significance of this cortical region's projections to the IC remains to be elucidated, the inputs to this cortical area are consistent with its function in learning and fear conditioning circuits of the brain. Together, these findings suggest that these layer 6 corticocollicular neurons form a distinct projection system to the IC. These layer 6 neurons may be one of the substrates by which the limbic system affects midbrain sound processing.

CHAPTER 4: LAYER 5 AND 6 CORTICOCOLLICULAR NEURONS PROVIDE CONTRASTING INNERVATION TO THE SUBDIVISIONS OF THE MOUSE IC

INTRODUCTION

The properties of corticofugal neurons are known to differ between layer 5 and layer 6 in other systems. Perhaps the most well-understood of these projections constitute the corticothalamic system. Corticothalamic layer 5 and layer 6 neurons possess distinct morphological, electrophysiological and network properties. Layer 6 corticothalamic systems comprise a large feedback system, and their axons from A1 and AAF primarily terminate in the ventral MGB. Layer 5 neurons from the same cortical areas project to higher-order thalamic nuclei, such as the dorsal MGB, and thus are hypothesized to play an important role in cortico-thalamo-cortical communication. Another notable difference between corticothalamic neurons from layers 5 and 6 is the size of the terminals at the level of the MGB. Layer 6 terminals are of type 1, generally not exceeding 2 μm in length along the long axis of the axon. Layer 5 terminals in the dorsal MGB are of type 2, which are significantly larger in size – 3 μm and above (Llano and Sherman 2008). These neuroanatomical differences are also correlated with specific electrophysiological properties for these neurons. While layer 6 neurons tend to fire in a tonic mode, layer 5 corticothalamic neurons may also fire a burst of action potentials upon hyperpolarization (Llano and Sherman 2009). More generally, layer 5 and layer 6 corticothalamic neurons have been hypothesized to have different roles in modulating the thalamus and supporting cortico-cortical communication (Ojima 1994, Guillery and Sherman 2002, Theyel, Llano et al. 2010).

More recently, similar differences were discovered in the IC of the mouse (Slater, Willis et al. 2013). Layer 5 corticocollicular neurons are pyramidal in morphology, with tall apical

dendrites reaching out to cortical layers 1 and 2. These neurons also exhibited burst firing mode, similar to bursting of layer 5 corticothalamic neurons. Layer 6 corticocollicular neurons' morphology was more difficult to classify. Often, their dendrites spanned across larger cortical areas, and these neurons tended to fire only in onset or tonic modes, with no bursting found.

Experiments in Chapter 3 described substantial heterogeneity within the corticocollicular system. Layer 6 corticocollicular neurons emanated from a wider area of the cortex with a non-auditory cortical component, while the majority of layer 5 corticocollicular neurons were confined to classical auditory regions such as A1, AAF, A2 and UF. These differences were also confirmed by the immunohistochemical findings, which showed that layer 5 corticocollicular neurons are located in cortical areas with higher levels of SMI32 and PV, both of which demarcate primary AC borders. However, the question of whether layer 5 and layer 6 corticocollicular neurons also innervate different subnuclei of the IC remains unknown.

Detailed functional and neuroanatomical descriptions of the three main subdivisions of the IC (CNIC, LCIC and DCIC) were provided in Chapter 1. It is important to reinstate here that CNIC is tonotopically organized and primarily involved in early processing of auditory information before it is routed to the MGB and the cortex. It has been shown to receive negligible corticotectal feedback. On the contrary, the LCIC and DCIC lack tonotopic gradients and are also the primary known targets of the corticocollicular neurons. Additionally, these two subdivisions receive input from multiple non-auditory brain structures, including those of the somatosensory and visual systems. It is unknown whether layer 5 and layer 6 corticocollicular neurons have similar projection patterns across all three subdivisions of the IC, or whether differential projection patterns at the level of the IC exist between these two layers. The answer to this question is important for understanding the nature of corticofugal influences on

information processing in the IC. Therefore, the aim of the experiments in this chapter was to examine the termination patterns of layer 5 and 6 corticocollicular neurons in the IC of the mouse.

METHODS

Animal Surgery and Tracer Injections

All surgical procedures were approved by the Institutional Animal Care and Use Committee at the University of Illinois at Urbana-Champaign. Animals were housed in animal care facilities approved by the American Association for Accreditation of Laboratory Animal Care (AAALAC). Rbp4-cre mouse line was successfully used by other researchers for selective labeling of layer 5 corticocollicular neurons. Adult (90-180 days old) Rbp4-cre male and female mice were used in this study. Additionally, 3 GAD67-GFP mice of similar age were used to examine the presence of corticocollicular terminals on GABAergic neurons of the IC.

Animals were anesthetized with ketamine hydrochloride (100 mg/kg) and xylazine (3 mg/kg) intraperitoneally and placed in a stereotaxic apparatus (David Kopf Instruments, Tujunga, CA). Aseptic conditions were maintained throughout the surgery. Following a small skin incision over the dorsal portion of the skull and resection of the temporalis muscle, a small craniotomy (0.5 mm in diameter) was created over the left AC. For injections into the IC, a small craniotomy (0.5 mm in diameter) was performed over the left IC (5.200 mm caudal to bregma and 1.200 mm left lateral from the sagittal suture). A new broken glass electrode (~20 μm tip diameter) was used for each injection using the following tracers.

For AAV injections, the left ACs of Rbp4-positive mice (n = 4) were injected with 250-500 nL of a mixture of equal concentrations of AAV9.CB7.CI.mCherry.WPRE.rBG (a Cre-independent virus) and AAV9.CAG.Flex.eGFP.WPRE.bGH (a virus only expressed in Cre+ cells), both at $3.43x10^{12}$ vg/mL, Penn Vector Core, Philadelphia, PA). For retrograde tracer injections into the cortex (n = 2), 250 nL of Alexa-594 conjugated cholera toxin subunit b (recombinant), CTb (0.5 % in PBS) (Thermo Fisher Scientific, Grand Island, NY) was pressure-injected for 5 min at the rate of 50 nl per/min.

The logic behind this experiment was as follows. Because the expression of the second virus containing eGFP is dependent on the presence of Cre, it could only be expressed in layer 5 corticocollicular neurons. The first construct will be expressed throughout the cortex, but since the only other projection to the IC arises from cortical layer 6, at the level of the IC, most of the mCherry (red) labeled terminals would mainly have to be coming from this layer. Therefore, at the level of the IC, two kinds of labeled terminals should predominate after expression is complete: yellow terminals (e.GFP + m.Cherry), which come from layer 5 neurons, and red terminals (m.Cherry) only, which arise from layer 6. Importantly, these two AAV9 viruses were identical in every regard in terms of their molecular biology; the only exceptions were differences in cre-dependence and fluorophore type.

Histological Processing

The animals were allowed to survive for two to three weeks, after which these the mice were first deeply anesthetized with a lethal intraperitoneal injection of ketamine hydrochloride (200 mg/kg) and xylazine (6 mg/kg), and then perfused transcardially with 4% paraformaldehyde

in phosphate-buffered saline (PBS) at pH 7.4. Frozen 50 µm sections were cut using a sliding microtome and collected in plastic section containers filled with PBS.

For immunohistochemistry, sections were washed 3 times for 5 minutes in PBS, microwaved for 15 seconds at full power for antigen retrieval, then incubated for 30 minutes in PBS containing 0.3% Triton-X (PBT) followed by a 30-minute long blocking step in a 3% serum containing PBT solution. Blocking serum was from the same species that the secondary antibody was generated in. Sections were then incubated with corresponding primary antibody overnight in the cold room. For NeuN staining, rabbit anti-NeuN antibody (Millipore Sigma, Burlington, MA) at 1:1000 dilution was used. Secondary antibody was diluted in the serum solution used for the primary wash and sections were incubated in this solution for 2 hours at room temperature. Alexa-633 conjugated secondary antibody was used (Invitrogen, Grand Island, NY). Then, the sections were washed in PBS three times for 10 minutes each, mounted on gelatin-coated slides, air-dried in dark room, coverslipped using fluorescence mounting medium (Vectashield H-1000, Vector labs) and sealed with nail polish.

Confocal Microscopy and Image Analysis

Confocal pictures were taken on a Leica SP8 UV/Visible Laser Confocal Microscope. 488 nm and 561 nm excitation were used for visualizing eGFP or GFP and mCherry, respectively. 633 nm excitation was used for visualizing NeuN-positive neurons. In order to get a look at individual corticocollicular terminals, 500 nm z-step was used, with the acquisition pixel size set to 0.141 µm in xy-plane. For the analysis, the areas of each terminal and en passant bouton were measured in ImageJ, blindly with respect to the subdivisions of the IC and cortical layers of origin. Two-sample Kolmogorov-Smirnov test was used to analyze the differences

between the distributions of layer-specific corticocollicular terminal size in each subnucleus of the IC.

RESULTS

First, Rbp4-cre mice were injected with equal concentration of two AAV9 viruses, as per descriptions in the methods section of this chapter. The expression of

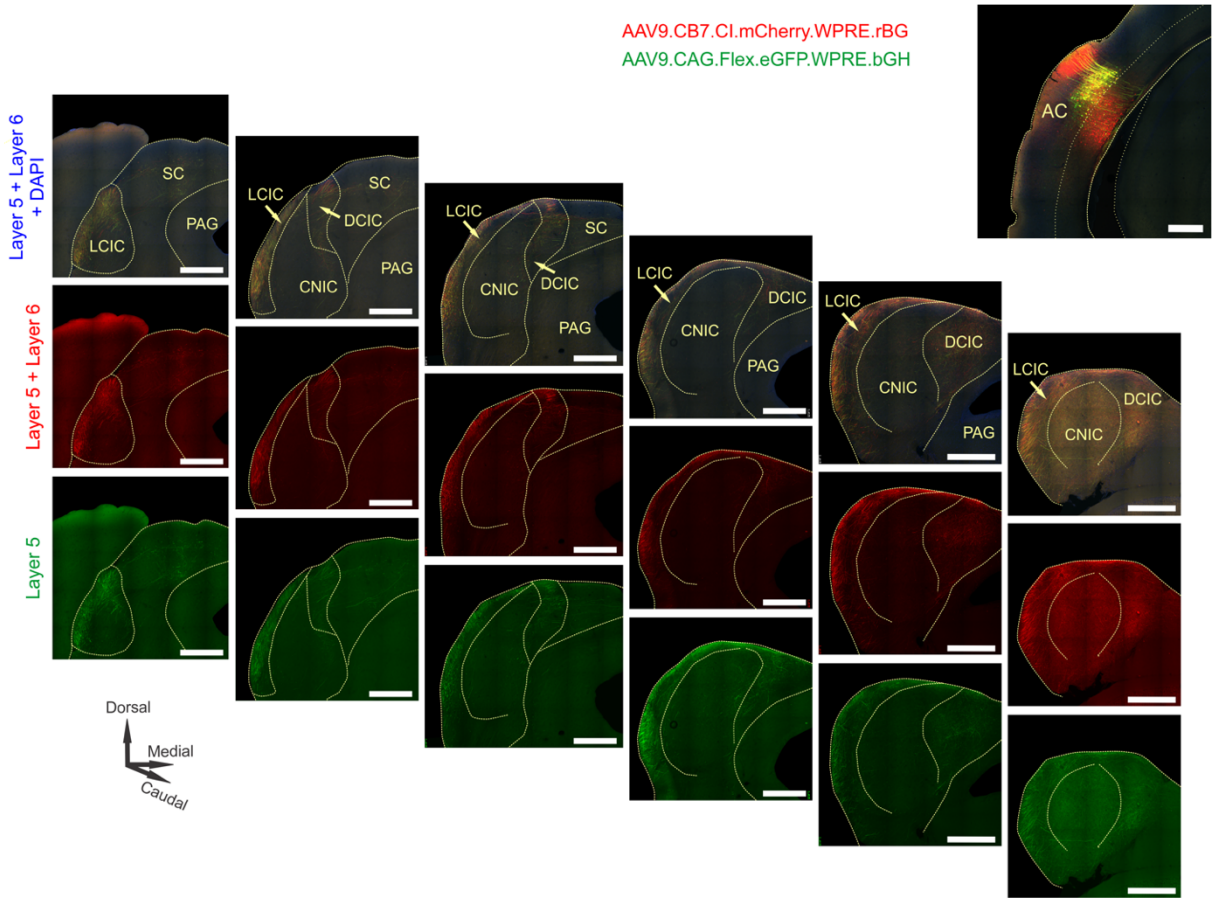

Figure 4.1. Corticocollicular termination patters at the level of the IC.
Both layer 5 and layer 6 corticocollicular terminals from the AC were densely distributed in the LCIC and DCIC. The green panel (e.GFP expression) shows layer 5 terminals only. The middle panel (m.Cherry) is a combined labeling of layers 5 and 6. The top panel shows the terminals from both layers. The yellow color is the labeling from layer 5, while purely red terminals are dominated by layer 6. Top right - injection site in the AC, with the dashed yellow line showing the border between cortical layers 5 and 6. Scale bar = 500 µm.

AAV9.CB7.CI.mCherry.WPRE.rBG spanned across all layers of the AC, while the expression of AAV9.CAG.Flex.eGFP.WPRE.bGH was restricted to layer 5 neurons only. Figure 4.1 displays a panel of coronal sections throughout the mouse IC with the patterns of expression. The AC injection site is shown in the top right corner. Consistent with numerous previous findings, the corticocollicular neurons primarily terminated in the DCIC and the LCIC. However, a difference was found in the CNIC. This tonotopically-organized subnucleus of the IC had a large number of and a different distribution of layer 5 terminals, but not layer 6 (two-sample Kolmogorov-Smirnov test, p-value = 5.032e-13) The overall distributions of layer 5 and 6 terminals did not vary significantly in the LCIC (two-sample Kolmogorov-Smirnov test, p-value = 0.2856), or the DCIC (two-sample Kolmogorov-Smirnov test, p-value = 0.06231). The distributions of terminal and bouton sizes are shown in figure 4.2. Interestingly, layer 5 corticocollicular terminals in the CNIC resembled a strong pattern of soma innervation (figure 4.3), where larger synaptic terminals tended to cluster in shapes that resemble neuronal somata.

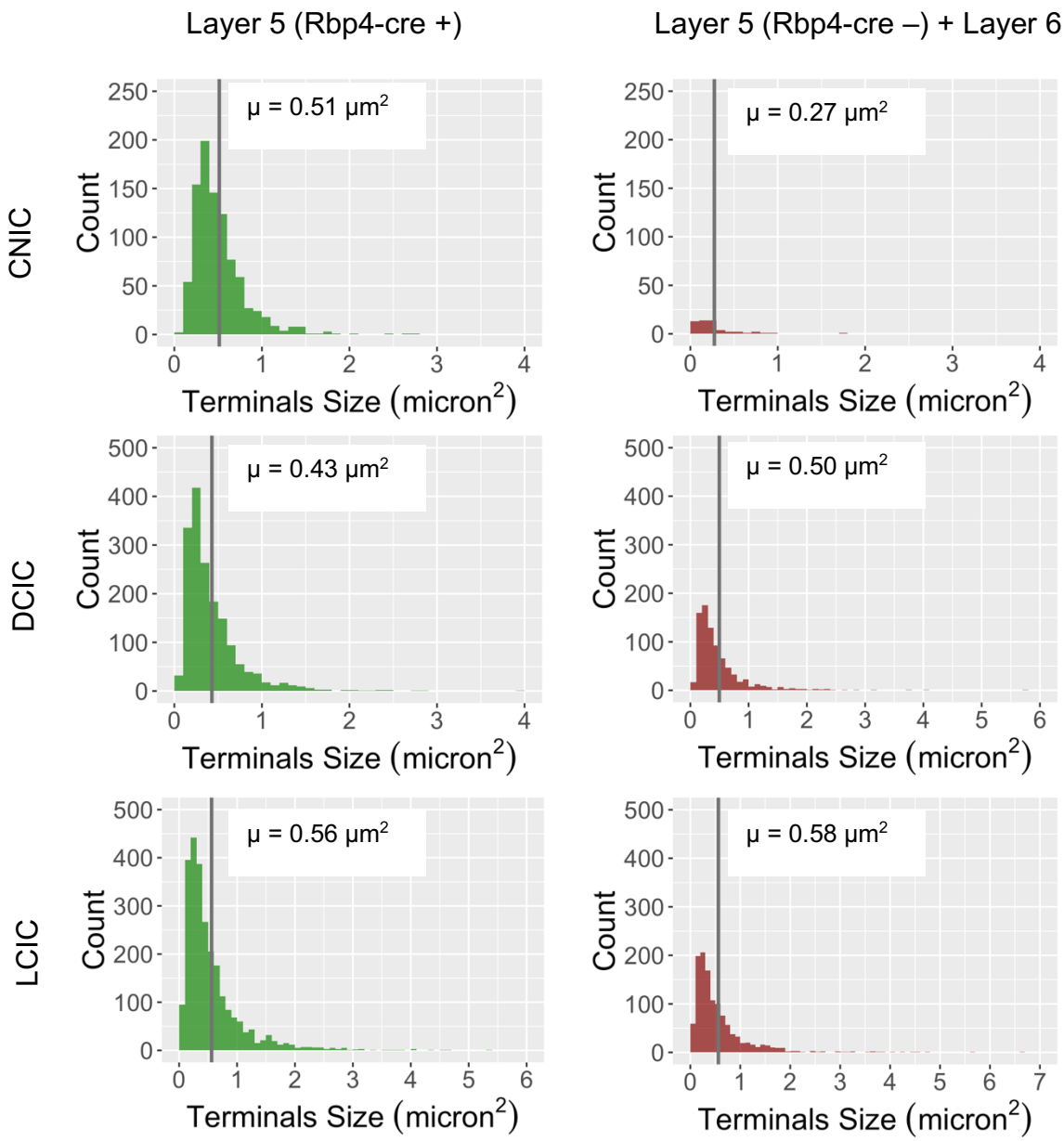

Figure 4.2. The distribution of size of layer 5 and layer 6 corticocollicular boutons and terminals in the main subdivisions of the mouse IC.
Each column represents the distributions of size for layer 5 (Rbp4-cre+) and layer 5 (Rbp4-cre –) + layer 6 corticocollicular boutons and terminals in the IC. The rows refer to each of the subnuclei of the IC. Grey vertical lines in each graph show the mean of the distribution.

Next, two more Rbp4-cre mice were used for same injections in the AC. After a two-week survival, the brain tissue from these animals was subjected to an immunostaining protocol

for NeuN, the details of which were described in the methods section for this chapter as well. Figure 4.4 shows the results of high-resolution confocal microscopy, which revealed that only layer 5 corticocollicular terminals were present on the CNIC cell bodies stained for NeuN – a commonly used neuronal marker (Wolf, Buslei et al. 1996, Lind, Franken et al. 2005, Korzhevskii, Gilerovich et al. 2006). This finding further supports the hypothesis that layer 5 and layer 6 corticocollicular terminals may exert differential effects in the IC.

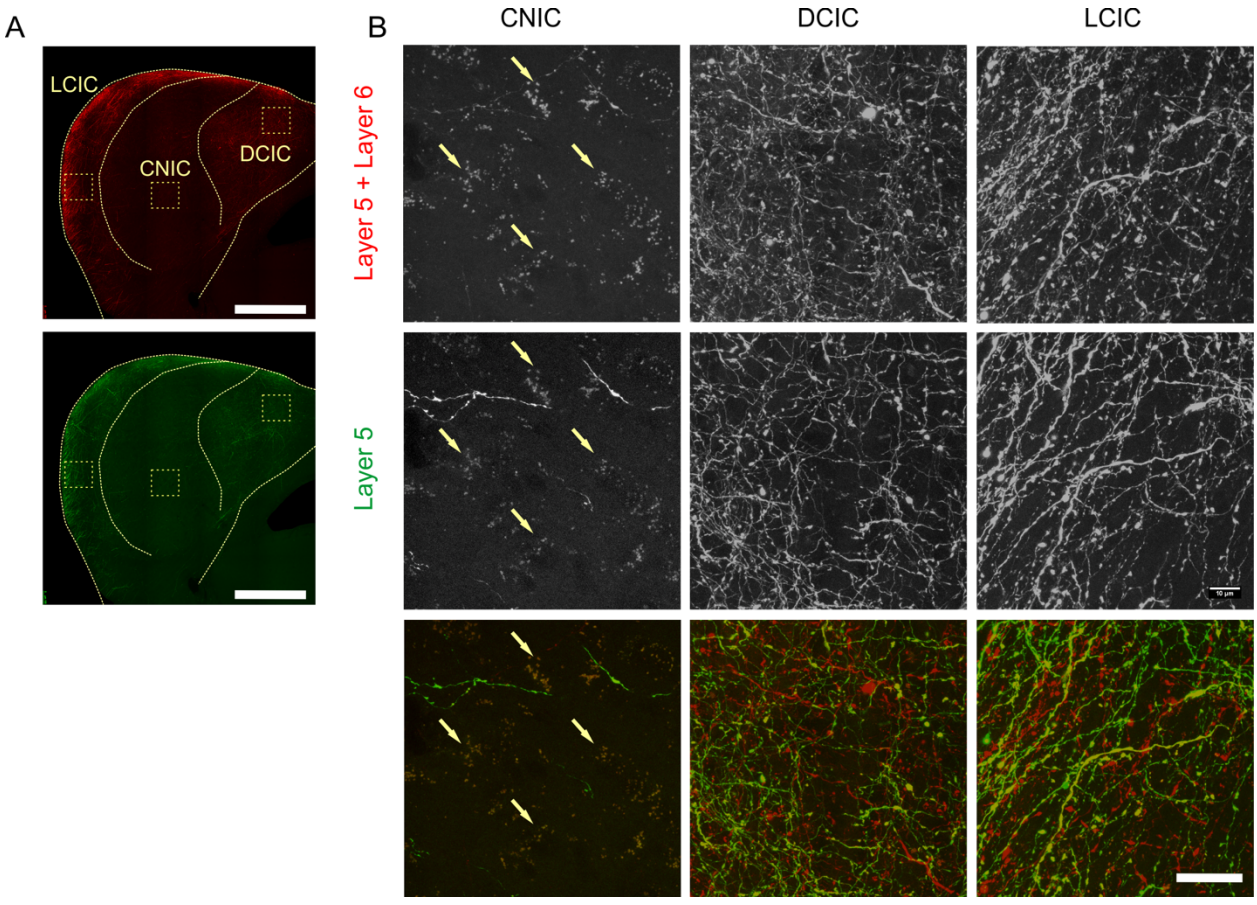

Figure 4.3. Details of the corticocollicular termination patterns in the subdivision of the IC.
(A) AAV9 expression in layer 6 + layer 5 and in layer 5 in the Rbp4 mouse. The insets are regions whose higher resolution details are shown in B. (B). Although the CNIC received significantly less corticocollicular input overall, consistent with previous findings, a number synaptic boutons (arrows pointing) emanating from layer 5 were found in this subdivision, while layer 6 boutons were virtually absent. Scale bar = 500 µm in (A) and 20 µm in (B).

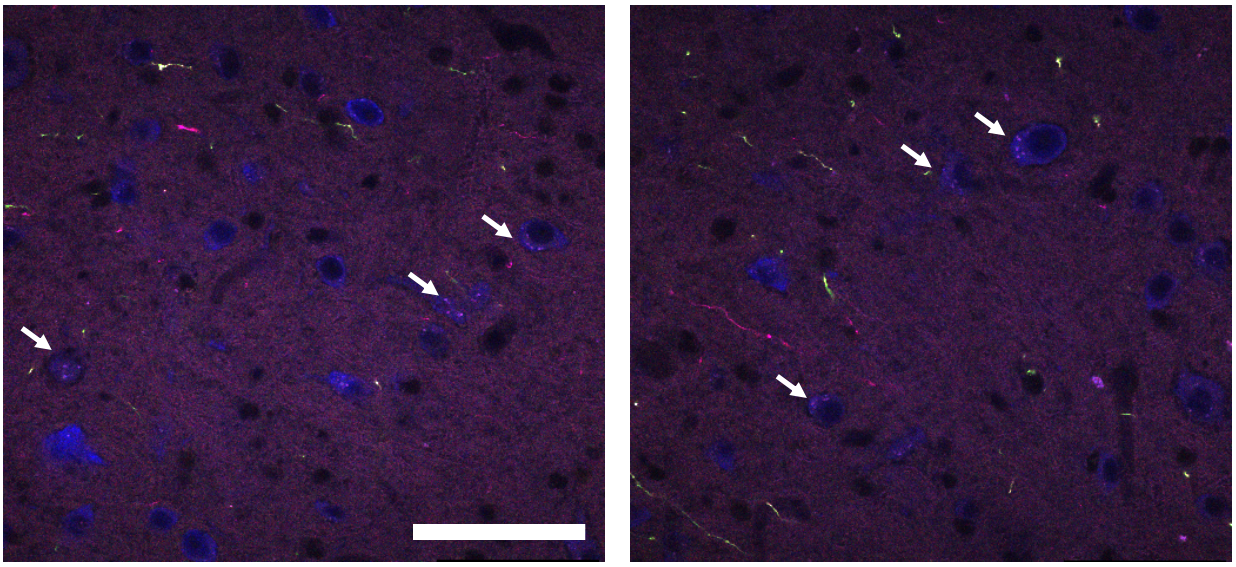

Figure 4.4. Layer 5 corticocollicular terminals contact the cell bodies of neurons in the CNIC.
A single slice of a confocal stack showing AAV9 expression in layer 6 + layer 5 and in layer 5 in the Rbp4 mouse CNIC stained for NeuN. Layer 5 axosomatic synaptic terminals (arrows pointing) were found in this subdivision of the IC. Scale bar = 50 μm. Z-step = 500 nm.

The CNIC, as well as other subdivisions of the IC, contain a large number of inhibitory GABAergic neurons (Ono, Yanagawa et al. 2005, Ito, Bishop et al. 2009). These GABAergic neurons have different morphological and electrophysiological properties, including a group of large GABAergic neurons that project to the MGB (Mellott, Foster et al. 2014). Some, but not all, GABAergic neurons in the CNIC also receive large glutamatergic axosomatic terminals (Ito, Bishop et al. 2009). Given these findings, and the importance of sources of inhibition in the IC (Casseday, Ehrlich et al. 1994), I set to examine the presence of layer 5 corticocollicular terminals on inhibitory (GABAergic) and excitatory (glutamatergic) neurons in the mouse IC. Building upon my previous findings from this chapter, AAV9.CB7.CI.mCherry.WPRE.rBG was injected in the left AC of three GAD67-GFP mice, and the distribution of labeled terminals at the level of the IC was examined through high-resolution confocal microscopy. The results of these injections are presented in figure 4.5. The corticocollicular terminals were found on both

GABAergic and non-GABAergic neurons. Since there is no known overlap between GABAergic and glutamatergic neurons in the brain, and only these two classes are present in the IC, by exclusion the non-GABAergic neurons must be glutamatergic in nature.

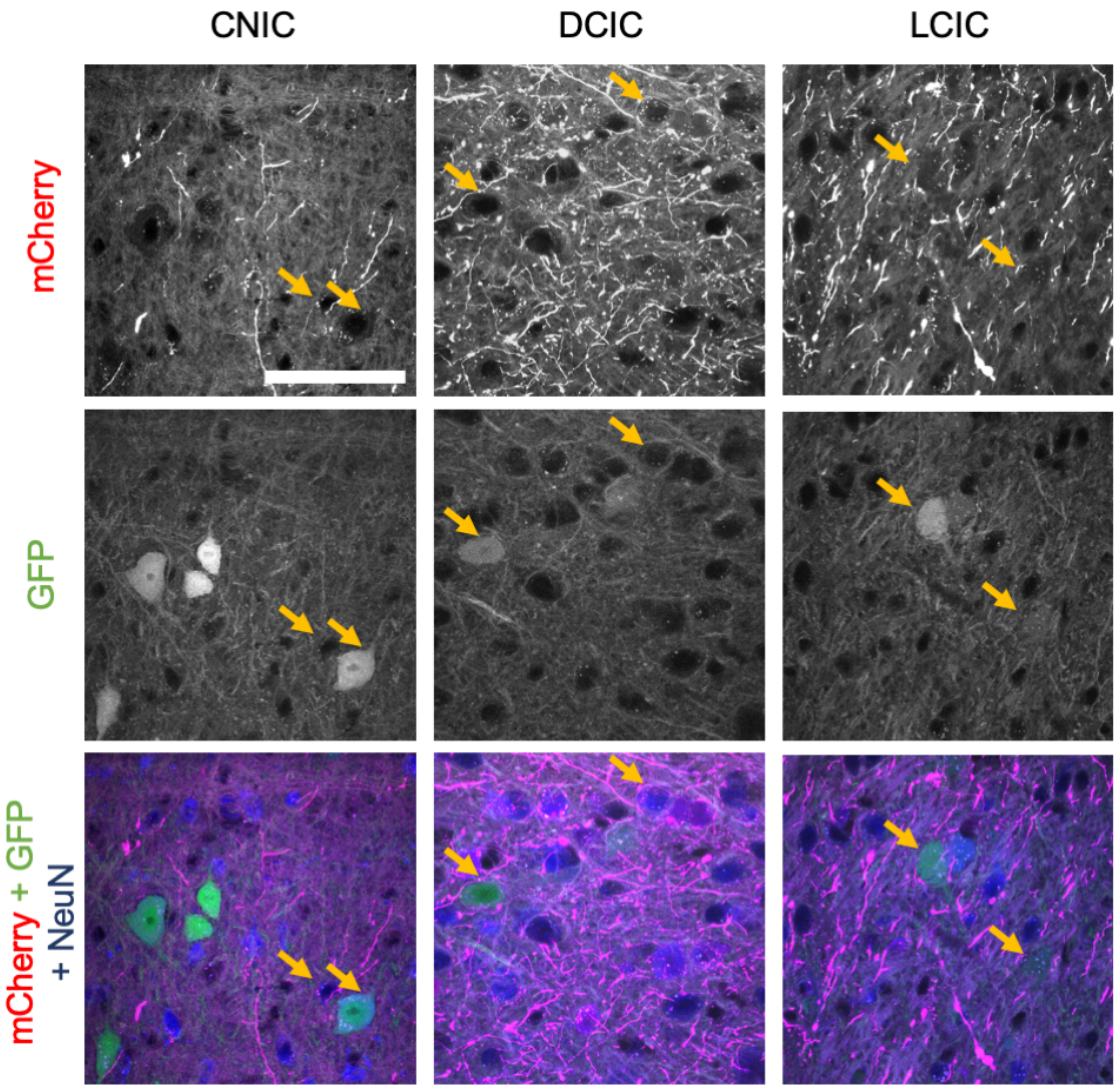

Figure 4.5. Corticocollicular neurons make direct contacts with GABAergic and glutamatergic neurons in the IC.
AAV9.mCherry expression the three main subdivisions of the IC in GAD67-GFP mouse. In the CNIC (left column), layer 5 terminal contact excitatory and inhibitory neurons. Yellow arrows are pointing to cells with co-localized labeled corticocollicular terminals. The corticocollicular neurons also make axosomatic contacts in the DCIC and LCIC (middle and right vertical panels). However, because both layer 5 and layer 6 corticocollicular neurons projects to these two subdivisions, further layer-specificity could not be deduced. Scale bar = 50 µm.

DISCUSSION

The results of this chapter's experiments showed that layer 5 and layer 6 corticocollicular neurons contact different populations of neurons in the mouse IC in a layer-specific fashion. Both layer 5 and layer 6 project to the DCIC and the LCIC, where they make different types of contacts, including axosomatic connections. These results are consistent with some recent findings, where strong, medium and weak types of excitatory corticocollicular synapses were described (Song, Lucaci et al. 2018). However, only layer 5 corticocollicular terminals were discovered in the CNIC. These corticocollicular neurons formed predominantly axosomatic contacts with both inhibitory and excitatory neurons of the IC. The presence of synaptic corticocollicular connections with inhibitory and excitatory neurons in the IC is also consistent with previous recent research findings (Chen, Cheng et al. 2018).

The method of combining two viral vectors that only differ in terms of the fluorophore and cre-dependence also proved to be informative and useful in achieving partial segregation of synaptic input from two neuronal populations of interest located in the same cortical region. Specifically, co-expression of cre-dependent vector AAV9.CAG.Flex.eGFP.WPRE.bGH and a non-specific vector AAV9.CB7.CI.mCherry.WPRE.rBG labeled layer 5 and layer 5 and 6 corticocollicular neurons, respectively. In this case, layer 5 Rpb4-positive neurons expressed both eGFP and mCherry, while layer 6 Rbp4-negative neurons only had the expression of mCherry. At the level of the IC, specifically in the CNIC, eGFP (green) and mCherry (red) co-localized in axosomatic synaptic terminals, suggesting that these terminals came from layer 5 corticocollicular neurons. In other subdivisions of the IC, both red and green terminals were found, as well as only red terminals, suggesting the presence of synapses formed by layer 5 as well as by layer 6 corticocollicular neurons.

Taken together, these neuroanatomical findings support the hypothesis that layer 5 and layer 6 corticocollicular neurons may play different roles in auditory processing in the IC. Given that layer 5 corticocollicular neurons form axosomatic connections with both excitatory and inhibitory neurons in the CNIC, their influences may be responsible for early changes in frequency and duration tuning observed in the CNIC following electrical stimulation of the AC in mice. The functional role of layer 6 corticocollicular neurons must be viewed in terms of their exclusive projections to DCIC and LCIC, where they may be involved in auditory and integrative multisensory processing.

Recently, another study showed that layer 5 Rbp4 neurons also send axonal branches to the auditory thalamus, as well as certain non-auditory brain structures including the striatum and the lateral amygdala (Asokan, Williamson et al. 2018). However, it is not known whether all layer 5 Rbp4-positive neurons that project to the IC also project to the thalamus, the striatum and the amygdala, or whether there is a specific subpopulation of layer 5 neurons that have the axonal branches innervating these multiple targets. Identifying and describing these connectivity patterns further will have important implications for our understanding of top-down systems in general and their role in auditory processing and plasticity.

CHAPTER 5: CONCLUSION

In this dissertation's experiments, it was demonstrated that multiple top-down streams exist within the corticocollicular system, all of which may differentially modulate information processing at the level of the IC. The heterogeneity described in this work could be responsible for the different functions assigned to the corticocollicular system, which were reviewed earlier in Chapter 1. To summarize the present findings briefly, layer 5 and layer 6 corticocollicular neurons comprise two distinct populations in the cortex, originate from many auditory and multisensory cortical areas, and innervate distinct subnuclei of the IC.

In Chapter 2, it was shown that the distributions of layer 5 and layer 6 corticocollicular neurons are partially but significantly non-overlapping with respect to each other and the cortical areas from which they originate. It was found that the IC receives heavy input from layer 6 from a cortical region rostral and ventral to the lemniscal AC, as indicated by staining for PV and SMI32. The centers and widths of layer 5 and layer 6 corticocollicular neuronal distributions were significantly different in the following manner: layer 6 corticocollicular neurons encompassed a broader area of the cortex than layer 5, and its distribution's center was shifted more rostrally and ventrally compared to layer 5. This organization implies that certain cortical areas modulate the IC either through layer 6 corticocollicular neurons or both layers 5 and 6.

The findings in Chapter 3 demonstrated that layer 5 and layer 6 corticocollicular neurons were differentially distributed with respect to functionally mapped areas of the mouse AC. More specifically, an area of the cerebral cortex located rostrally and ventrally to the mouse AC contained only layer 6 corticocollicular neurons, and this cortical region did not respond to sound stimuli such as pure tones of different frequencies, neither was it responsive to more ethologically relevant sounds such as species-specific (mouse) calls. Moreover, it did not receive

any input from any subdivisions of the MGB, further confirming that it is not an auditory region of the cortex. Instead, the connectivity of this region with the thalamus and the amygdala points to its role in limbic and multisensory functions.

Chapter 4 examined the termination patterns from layer 5 and 6 corticocollicular neurons at the level of the IC. With respect to the three subnuclei of the IC, certain contrasting distributions of axonal terminals were observed. While both layer 5 and layer 6 projected to the DCIC and the LCIC, only layer 5 terminals were discovered in the CNIC. These layer 5 terminals appeared to be mainly axosomatic and synapsed onto both GABAergic and glutamatergic neurons of the CNIC.

A few discussion points to be raised regarding the results of this work. Despite the large and heterogeneous distributions of IC injection sites in Chapter 2, similar differences between layer 5 and layer 6 corticocollicular projections were seen. The presence of labeled layer 6 corticocollicular neurons in the cortical regions located rostro-caudally to AC was observed even when injection sites were small and located in different subnuclei of the IC. This finding suggests that layer 6 corticocollicular neurons more broadly innervate the IC compared to layer 5. The precise functional significance of these termination patterns is yet to be determined; however, I propose that these layer 6 neurons may be involved in some global context-dependent modulation of auditory signals that reach the midbrain through the ascending pathways. Their wider distribution in the cortex also suggests that they would be better suited for integrating neural signals from other modalities and relaying this integrated or multisensory information to the colliculus. In line with this hypothesis, a recent study in the visual system found that ablation of deep layer 6 neurons in secondary visual cortex of the rat (V2) resulted in complete loss of visual object recognition memory (López-Aranda, López-Téllez et al. 2009). It is possible that

layer 6 corticocollicular cells play a similar role in the auditory system for auditory object recognition. In fact, it is possible that learning deficits observed in (Bajo, Nodal et al. 2010) were fully or partially due to the ablation of layer 6 corticocollicular neurons.

Although no acoustically-driven responses were found in the corticocollicular layer-6-rich rostroventral region of the temporal cortex, one might argue that imaging in awake animals may have shown different results. However, the maps in Chapter 3 were similar to the distributions of acoustically-responsive areas seen in many of the previous studies with different anesthetics, level of anesthesia, and imaging or recording modalities (Stiebler, Neulist et al. 1997, Tohmi, Takahashi et al. 2009, Hackett, Barkat et al. 2011, Issa, Haeffele et al. 2014, Kato, Gillet et al. 2015, Tsukano, Horie et al. 2015). In this dissertation, four regions of the mouse AC could be distinguished based on their responses to pure tones. A1 and AAF were tonotopically organized. The pure tones of ultrasonic frequencies activated neurons in the UF, while all pure tone stimuli also activated A2, located ventrally to A1 and AAF gradient convergence. These regions overlapped more so with the distributions of layer 5 corticocollicular neurons, and less so with the corticocollicular neurons emanating from layer 6. Additionally, four types of mouse-specific calls used in this study activated neurons located primarily in A2. Again, this activation did not overlap with the cortical area containing only layer 6 but not layer 5 corticocollicular cells. Consistent with its imaging responses, this corticocollicular layer-6 area of the mouse cortex did not receive input from any subdivisions of the MGB. The finding distinguishes this region from the insular auditory field, which received input from the ventral division of the MGB (Takemoto, Hasegawa et al. 2014). Instead, intralaminar nuclei were the main source of thalamic input to this area. The lateral nucleus of the amygdala also sent a heavy projection to this area. Together, these results suggest that layer 6 corticocollicular neurons are better positioned to send

a broad spectrum of multisensory and limbic information to the IC, potentially to modulate IC function in response to multisensory and behaviorally-relevant stimuli (Aitkin, Dickhaus et al. 1978, Holmstrom, Eeuwes et al. 2010).

Consistent with previous findings (Herbert, Aschoff et al. 1991, Budinger, Heil et al. 2000, Bajo, Nodal et al. 2007), in the current work layer 5 corticocollicular neurons also appeared to be confined to tonotopically-organized lemniscal auditory fields (A1 and AAF) as confirmed by PV and SMI-32 immunostaining and imaging. Rbp4-cre layer 5 corticocollicular neurons also exhibited axosomatic patters on innervation in the CNIC. In contrast to layer 5, layer 6 terminals were not found in this subdivision of the IC. Thus, layer 5 corticocollicular neurons may be the main drivers of frequency shifts and changes in tuning duration observed in the IC upon AC stimulation. The innervation patterns discovered in this dissertation are consistent with the strong effects observed at the level of the IC when the cortex is stimulated (Yan and Suga 1998, Ma and Suga 2001). It is worth to note that not all layer 5 corticocollicular neurons are Rbp4-positive (Xiong, Liang et al. 2015), while only these neurons were found to project to the CNIC. Consequently, another class of layer 5 corticocollicular neurons is Rbp4-negative, and these neurons project either to DCIC or LCIC or both. Although the methods used in this work could not distinguish between those three possibilities, it is clear that Rbp4-negative layer 5 neurons comprise yet another unique top-down projection embedded within the corticocollicular system. Layer 6 corticocollicular terminals were only found in the DCIC and LCIC. Both of these IC subdivisions receive significant input from other sensory modalities. Multisensory responses have also been described in these subdivisions previously, which was reviewed in Chapter 1. Layer 6 projection patterns in the IC remain consistent with the overarching hypothesis for their multisensory function.

Both layer 5 and layer 6 corticocollicular projections have been found across multiple species (Games and Winer 1988, Künzle 1995, Schofield 2009, Bajo and King 2012, Lesicko, Hristova et al. 2016), suggesting their general importance in top-down modulation of auditory processing. This dissertation described significant heterogeneity within the corticocollicular system, showing the presence of multiple top-down streams. The exact physiological and behavioral significance of these neuroanatomical finding will still need to be addressed in future research. The summary of the main findings is presented in figure 5.1.

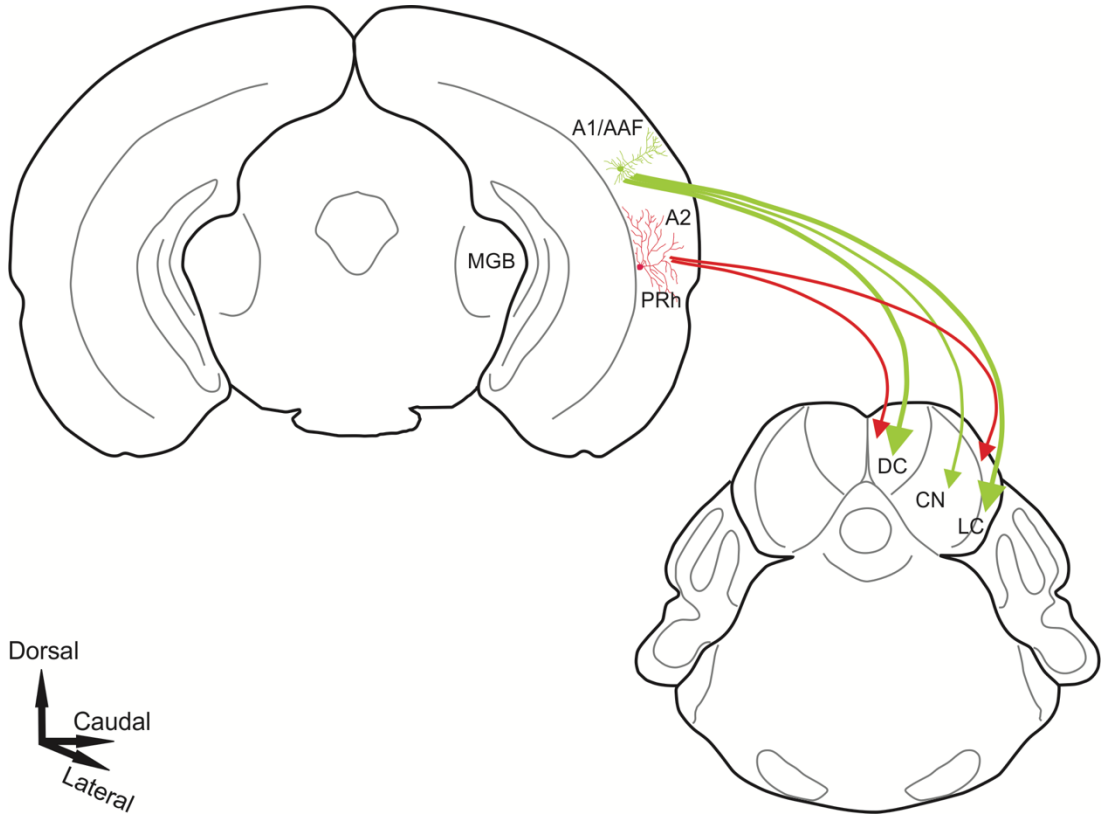

Figure 5.1. A schematic representation of the corticocollicular projections in the mouse. Layer 5 corticocollicular neurons are mainly located in A1 and AAF, and project to all three subdivisions of the IC, namely DC (DCIC), CN (CNIC) and LC (LCIC). The majority of layer 6 corticocollicular neurons reside in A2 and perirhinal areas (PRh), and their projections were only found in non-lemniscal subdivisions – LC and DC. Layer 6 corticocollicular neurons comprised a much broader population in the cortex, while layer 5 corticocollicular neurons were mainly confined to A1 and AAF areas of the cortex.

REFERENCES

1. Abercrombie, M. (1946). "Estimation of nuclear population from microtome sections." The Anatomical Record **94**(2): 239-247.

2. Aitkin, L., H. Dickhaus, W. Schult and M. Zimmermann (1978). "External nucleus of inferior colliculus: auditory and spinal somatosensory afferents and their interactions." Journal of Neurophysiology **41**(4): 837-847.

3. Andersen, R. A., R. L. Snyder and M. M. Merzenich (1980). "The topographic organization of corticocollicular projections from physiologically identified loci in the AI, AII, and anterior auditory cortical fields of the cat." Journal of Comparative Neurology **191**(3): 479-494.

4. Anderson, L. and M. Malmierca (2013). "The effect of auditory cortex deactivation on stimulus‐specific adaptation in the inferior colliculus of the rat." European Journal of Neuroscience **37**(1): 52-62.

5. Asokan, M. M., R. S. Williamson, K. E. Hancock and D. B. Polley (2018). "Sensory overamplification in layer 5 auditory corticofugal projection neurons following cochlear nerve synaptic damage." Nature Communications **9**(1): 2468.

6. Bajo, V. M. and A. J. King (2012). "Cortical modulation of auditory processing in the midbrain." Front Neural Circuits **6**: 114.

7. Bajo, V. M., F. R. Nodal, J. K. Bizley, D. R. Moore and A. J. King (2007). "The ferret auditory cortex: descending projections to the inferior colliculus." Cerebral Cortex **17**(2): 475-491.

8. Bajo, V. M., F. R. Nodal, D. R. Moore and A. J. King (2010). "The descending corticocollicular pathway mediates learning-induced auditory plasticity." Nat Neurosci **13**(2): 253-260.

9. Budinger, E., P. Heil and H. Scheich (2000). "Functional organization of auditory cortex in the Mongolian gerbil (Meriones unguiculatus). IV. Connections with anatomically characterized subcortical structures." European Journal of Neuroscience **12**(7): 2452-2474.

10. Casseday, J., D. Ehrlich and E. Covey (1994). "Neural tuning for sound duration: role of inhibitory mechanisms in the inferior colliculus." Science **264**(5160): 847-850.

11. Casseday, J. H., T. Fremouw and E. Covey (2002). The Inferior Colliculus: A Hub for the Central Auditory System. Integrative Functions in the Mammalian Auditory Pathway. D. Oertel, R. R. Fay and A. N. Popper. New York, NY, Springer New York**:** 238-318.

12. Caviness, V. S. (1975). "Architectonic map of neocortex of the normal mouse." Journal of Comparative Neurology **164**(2): 247-263.

13. Chen, C., M. Cheng, T. Ito and S. Song (2018). "Neuronal Organization in the Inferior Colliculus Revisited with Cell-Type-Dependent Monosynaptic Tracing." J Neurosci **38**(13): 3318-3332.

14. Chernock, M. L., D. T. Larue and J. A. Winer (2004). "A periodic network of neurochemical modules in the inferior colliculus." Hearing research **188**(1-2): 12-20.

15. Cruikshank, S., H. Killackey and R. Metherate (2001). "Parvalbumin and calbindin are differentially distributed within primary and secondary subregions of the mouse auditory forebrain." Neuroscience **105**(3): 553-569.

16. Davis, M. H. and I. S. Johnsrude (2007). "Hearing speech sounds: top-down influences on the interface between audition and speech perception." Hearing research **229**(1): 132-147.

17. Davis, M. H., I. S. Johnsrude, A. Hervais-Adelman, K. Taylor and C. McGettigan (2005). "Lexical information drives perceptual learning of distorted speech: evidence from the comprehension of noise-vocoded sentences." Journal of Experimental Psychology: General **134**(2): 222.

18. Ehret, R. (1997). The central auditory system, Oxford University Press, USA.

19. Games, K. D. and J. A. Winer (1988). "Layer V in rat auditory cortex: projections to the inferior colliculus and contralateral cortex." Hearing research **34**(1): 1-25.

20. Grimsley, J., J. Monaghan and J. J. Wenstrup (2011). "Development of social vocalizations in mice." PloS one **6**(3): e17460-e17460.

21. Grimsley, J. M., S. Sheth, N. Vallabh, C. A. Grimsley, J. Bhattal, M. Latsko, A. Jasnow and J. J. Wenstrup (2016). "Contextual Modulation of Vocal Behavior in Mouse: Newly Identified 12 kHz "Mid-Frequency" Vocalization Emitted during Restraint." Front Behav Neurosci **10**: 38.

22. Guillery, R. and S. M. J. N. Sherman (2002). "Thalamic relay functions and their role in corticocortical communication: generalizations from the visual system." **33**(2): 163-175.

23. Hackett, T. A., T. R. Barkat, B. M. O'Brien, T. K. Hensch and D. B. Polley (2011). "Linking topography to tonotopy in the mouse auditory thalamocortical circuit." The Journal of Neuroscience **31**(8): 2983-2995.

24. Halassa, M. M., J. H. Siegle, J. T. Ritt, J. T. Ting, G. Feng and C. I. Moore (2011). "Selective optical drive of thalamic reticular nucleus generates thalamic bursts and cortical spindles." Nat Neurosci **14**(9): 1118-1120.

25. Herbert, H., A. Aschoff and J. Ostwald (1991). "Topography of projections from the auditory cortex to the inferior colliculus in the rat." Journal of Comparative Neurology **304**(1): 103-122.

26. Hofstetter, K. M. and G. Ehret (1992). "The auditory cortex of the mouse: Connections of the ultrasonic field." Journal of Comparative Neurology **323**(3): 370-386.

27. Holmstrom, L. A., L. B. Eeuwes, P. D. Roberts and C. V. Portfors (2010). "Efficient encoding of vocalizations in the auditory midbrain." J Neurosci **30**(3): 802-819.

28. Honma, Y., H. Tsukano, M. Horie, S. Ohshima, M. Tohmi, Y. Kubota, K. Takahashi, R. Hishida, S. Takahashi and K. Shibuki (2013). "Auditory cortical areas activated by slow frequency-modulated sounds in mice." PLoS One **8**(7): e68113.

29. Horie, M., H. Tsukano, R. Hishida, H. Takebayashi and K. Shibuki (2013). "Dual compartments of the ventral division of the medial geniculate body projecting to the core region of the auditory cortex in C57BL/6 mice." Neurosci Res **76**(4): 207-212.

30. Horie, M., H. Tsukano, H. Takebayashi and K. Shibuki (2015). "Specific distribution of non-phosphorylated neurofilaments characterizing each subfield in the mouse auditory cortex." Neurosci Lett **606**: 182-187.

31. Issa, J. B., B. D. Haeffele, A. Agarwal, D. E. Bergles, E. D. Young and D. T. Yue (2014). "Multiscale optical Ca 2+ imaging of tonal organization in mouse auditory cortex." Neuron **83**(4): 944-959.

32. Ito, T., D. C. Bishop and D. L. Oliver (2009). "Two classes of GABAergic neurons in the inferior colliculus." J Neurosci **29**(44): 13860-13869.

33. Joachimsthaler, B., M. Uhlmann, F. Miller, G. Ehret and S. Kurt (2014). "Quantitative analysis of neuronal response properties in primary and higher-order auditory cortical fields of awake house mice (Mus musculus)." Eur J Neurosci **39**(6): 904-918.

34. Kato, H. K., S. N. Gillet and J. S. Isaacson (2015). "Flexible Sensory Representations in Auditory Cortex Driven by Behavioral Relevance." Neuron **88**(5): 1027-1039.

35. Korzhevskii, D., E. Gilerovich, N. Zin'kova, I. Grigor'ev and V. Otellin (2006). "Immunocytochemical detection of brain neurons using the selective marker NeuN." Neuroscience and behavioral physiology **36**(8): 857-859.

36. Künzle, H. J. C. C. (1995). "Regional and laminar distribution of cortical neurons projecting to either superior or inferior colliculus in the hedgehog tenrec." **5**(4): 338-352.

37. Lee, C., C. Schreiner, K. Imaizumi and J. Winer (2004). "Tonotopic and heterotopic projection systems in physiologically defined auditory cortex." Neuroscience **128**(4): 871-887.

38. Lee, C. C. and J. A. Winer (2011). "Convergence of thalamic and cortical pathways in cat auditory cortex." Hear Res **274**(1-2): 85-94.

39. Lesicko, A. M., T. S. Hristova, K. C. Maigler and D. A. Llano (2016). "Connectional Modularity of Top-Down and Bottom-Up Multimodal Inputs to the Lateral Cortex of the Mouse Inferior Colliculus." J Neurosci **36**(43): 11037-11050.

40. Lind, D., S. Franken, J. Kappler, J. Jankowski and K. Schilling (2005). "Characterization of the neuronal marker NeuN as a multiply phosphorylated antigen with discrete subcellular localization." Journal of neuroscience research **79**(3): 295-302.

41. Llano, D. A. and S. M. Sherman (2008). "Evidence for nonreciprocal organization of the mouse auditory thalamocortical–corticothalamic projection systems." Journal of Comparative Neurology **507**(2): 1209-1227.

42. Llano, D. A. and S. M. Sherman (2009). "Differences in intrinsic properties and local network connectivity of identified layer 5 and layer 6 adult mouse auditory corticothalamic neurons support a dual corticothalamic projection hypothesis." Cerebral Cortex: bhp050.

43. López-Aranda, M. F., J. F. López-Téllez, I. Navarro-Lobato, M. Masmudi-Martín, A. Gutiérrez and Z. U. Khan (2009). "Role of Layer 6 of V2 Visual Cortex in Object-Recognition Memory." Science **325**(5936): 87.

44. Lotto, A. J. and K. R. Kluender (1998). "General contrast effects in speech perception: Effect of preceding liquid on stop consonant identification." Perception & Psychophysics **60**(4): 602-619.

45. Ma, X. and N. Suga (2001). "Corticofugal modulation of duration-tuned neurons in the midbrain auditory nucleus in bats." Proceedings of the National Academy of Sciences **98**(24): 14060-14065.

46. Malmierca, M. S., M. A. Merchán, C. K. Henkel and D. L. Oliver (2002). "Direct projections from cochlear nuclear complex to auditory thalamus in the rat." Journal of Neuroscience **22**(24): 10891-10897.

47. Malmierca, M. S. and D. K. Ryugo (2012). "Auditory System." 607-645.

48. Masterton, R. (1992). "Role of the central auditory system in hearing: the new direction." Trends in neurosciences **15**(8): 280-285.

49. McMains, S. and S. Kastner (2011). "Interactions of top-down and bottom-up mechanisms in human visual cortex." J Neurosci **31**(2): 587-597.

50. Meininger, V., D. Pol and P. Derer (1986). "The inferior colliculus of the mouse. A Nissl and Golgi study." Neuroscience **17**(4): 1159-1179.

51. Mellott, J. G., N. L. Foster, K. T. Nakamoto, S. D. Motts and B. R. Schofield (2014). "Distribution of GABAergic cells in the inferior colliculus that project to the thalamus." Front Neuroanat **8**: 17.

52. Mellott, J. G., E. Van der Gucht, C. C. Lee, A. Carrasco, J. A. Winer and S. G. Lomber (2010). "Areas of cat auditory cortex as defined by neurofilament proteins expressing SMI-32." Hearing research **267**(1): 119-136.

53. Nakamoto, K. T., T. M. Shackleton and A. R. Palmer (2010). "Responses in the inferior colliculus of the guinea pig to concurrent harmonic series and the effect of inactivation of descending controls." Journal of neurophysiology **103**(4): 2050-2061.

54. O'Connor, D. H., M. M. Fukui, M. A. Pinsk and S. Kastner (2002). "Attention modulates responses in the human lateral geniculate nucleus." Nat Neurosci **5**(11): 1203-1209.

55. Ojima, H. and K. Murakami (2011). "Triadic synaptic interactions of large corticothalamic terminals in non-lemniscal thalamic nuclei of the cat auditory system." Hearing research **274**(1): 40-47.

56. Ojima, H. J. C. C. (1994). "Terminal morphology and distribution of corticothalamic fibers originating from layers 5 and 6 of cat primary auditory cortex." **4**(6): 646-663.

57. Ono, M., Y. Yanagawa and K. Koyano (2005). "GABAergic neurons in inferior colliculus of the GAD67-GFP knock-in mouse: electrophysiological and morphological properties." Neurosci Res **51**(4): 475-492.

58. Patel, M. B., S. Sons, G. Yudintsev, A. M. Lesicko, L. Yang, G. A. Taha, S. M. Pierce and D. A. Llano (2017). "Anatomical characterization of subcortical descending projections to the inferior colliculus in mouse." J Comp Neurol **525**(4): 885-900.

59. Perales, M., J. A. Winer and J. J. Prieto (2006). "Focal projections of cat auditory cortex to the pontine nuclei." Journal of Comparative Neurology **497**(6): 959-980.

60. Ratzlaff, E. H. and A. Grinvald (1991). "A tandem-lens epifluorescence macroscope: hundred-fold brightness advantage for wide-field imaging." Journal of neuroscience methods **36**(2): 127-137.

61. Reichova, I. and S. M. Sherman (2004). "Somatosensory corticothalamic projections: distinguishing drivers from modulators." Journal of Neurophysiology **92**(4): 2185-2197.

62. Remez, R., P. Rubin, D. Pisoni and T. Carrell (1981). "Speech perception without traditional speech cues." Science **212**(4497): 947-949.

63. Scalf, P. E. and D. M. Beck (2010). "Competition in visual cortex impedes attention to multiple items." J Neurosci **30**(1): 161-169.

64. Schofield, B. R. (2009). "Projections to the inferior colliculus from layer VI cells of auditory cortex." Neuroscience **159**(1): 246-258.

65. Skoe, E. and N. Kraus (2010). "Hearing it again and again: on-line subcortical plasticity in humans." PLoS One **5**(10): e13645.

66. Slater, B. J., S. K. Sons, G. Yudintsev, C. M. Lee and D. A. Llano (2019). "Thalamocortical and Intracortical Inputs Differentiate Layer-Specific Mouse Auditory Corticocollicular Neurons." J Neurosci **39**(2): 256-270.

67. Slater, B. J., A. M. Willis and D. A. Llano (2013). "Evidence for layer-specific differences in auditory corticocollicular neurons." Neuroscience **229**: 144-154.

68. Song, J. H., D. Lucaci, I. Calangiu, M. T. C. Brown, J. S. Park, J. Kim, S. G. Brickley and P. Chadderton (2018). "Combining mGRASP and Optogenetics Enables High-Resolution Functional Mapping of Descending Cortical Projections." Cell Rep **24**(4): 1071-1080.

69. Stebbings, K. A., A. M. Lesicko and D. A. Llano (2014). "The auditory corticocollicular system: molecular and circuit-level considerations." Hear Res **314**: 51-59.

70. Stiebler, I., R. Neulist, I. Fichtel and G. Ehret (1997). "The auditory cortex of the house mouse: left-right differences, tonotopic organization and quantitative analysis of frequency representation." Journal of Comparative Physiology A **181**(6): 559-571.

71. Suzuki, W. A. (1996). "The anatomy, physiology and functions of the perirhinal cortex." Current opinion in neurobiology **6**(2): 179-186.

72. Takemoto, M., K. Hasegawa, M. Nishimura and W. J. Song (2014). "The insular auditory field receives input from the lemniscal subdivision of the auditory thalamus in mice." Journal of Comparative Neurology **522**(6): 1373-1389.

73. Terreros, G. and P. H. Delano (2015). "Corticofugal modulation of peripheral auditory responses." Front Syst Neurosci **9**: 134.

74. Theyel, B. B., D. A. Llano and S. M. Sherman (2010). "The corticothalamocortical circuit drives higher-order cortex in the mouse." Nature neuroscience **13**(1): 84-88.

75. Tohmi, M., K. Takahashi, Y. Kubota, R. Hishida and K. Shibuki (2009). "Transcranial flavoprotein fluorescence imaging of mouse cortical activity and plasticity." J Neurochem **109 Suppl 1**: 3-9.

76. Tsukano, H., M. Horie, T. Bo, A. Uchimura, R. Hishida, M. Kudoh, K. Takahashi, H. Takebayashi and K. Shibuki (2015). "Delineation of a frequency-organized region isolated from the mouse primary auditory cortex." Journal of neurophysiology **113**(7): 2900-2920.

77. Winer, J. A. (2005). "Decoding the auditory corticofugal systems." Hearing research **207**(1): 1-9.

78. Winer, J. A., M. L. Chernock, D. T. Larue and S. W. Cheung (2002). "Descending projections to the inferior colliculus from the posterior thalamus and the auditory cortex in rat, cat, and monkey." Hearing research **168**(1): 181-195.

79. Wise, S. and E. Jones (1977). "Cells of origin and terminal distribution of descending projections of the rat somatic sensory cortex." Journal of Comparative Neurology **175**(2): 129-157.

80. Wolf, H. K., R. Buslei, R. Schmidt-Kastner, P. K. Schmidt-Kastner, T. Pietsch, O. D. Wiestler and I. Blümcke (1996). "NeuN: a useful neuronal marker for diagnostic histopathology." Journal of Histochemistry & Cytochemistry **44**(10): 1167-1171.

81. Wood, N. L. and N. Cowan (1995). "The Cocktail Party Phenomenon Revisited: Attention and Memory in the Classic Selective Listening Procedure of Cherry (1953)." Journal of Experimental Psychology: General **124**(3): 243-262.

82. Xiong, X. R., F. Liang, B. Zingg, X. Y. Ji, L. A. Ibrahim, H. W. Tao and L. I. Zhang (2015). "Auditory cortex controls sound-driven innate defense behaviour through corticofugal projections to inferior colliculus." Nat Commun **6**: 7224.

83. Yan, J. and G. Ehret (2001). "Corticofugal reorganization of the midbrain tonotopic map in mice." Neuroreport **12**(15): 3313-3316.

84. Yan, J., Y. Zhang and G. Ehret (2005). "Corticofugal shaping of frequency tuning curves in the central nucleus of the inferior colliculus of mice." Journal of Neurophysiology **93**(1): 71-83.

85. Yan, W. and N. Suga (1998). "Corticofugal modulation of the midbrain frequency map in the bat auditory system." Nature neuroscience **1**(1): 54-58.

86. Zhang, G. W., W. J. Sun, B. Zingg, L. Shen, J. He, Y. Xiong, H. W. Tao and L. I. Zhang (2017). "A Non-canonical Reticular-Limbic Central Auditory Pathway via Medial Septum Contributes to Fear Conditioning." Neuron.

87. Zingg, B., X. L. Chou, Z. G. Zhang, L. Mesik, F. Liang, H. W. Tao and L. I. Zhang (2017). "AAV-Mediated Anterograde Transsynaptic Tagging: Mapping Corticocollicular Input-Defined Neural Pathways for Defense Behaviors." Neuron **93**(1): 33-47.